Test Plan for Millimeter-Wave Wireless Device Over-the-Air Performance

Version 1.0.1

April 2020

Use Instructions

All testing to this test plan must be conducted in a CTIA Authorized Test Lab. This may be accomplished in one of two ways:

1. As part of a PTCRB certification request submitted at https://www.ptcrb.com/
2. By submitting an OTA Test Plan use request at https://ctiacert.org/

CTIA Certification LLC
1400 16th Street, NW
Suite 600
Washington, DC 20036

1.202.785.0081

programs@ctiacertification.org

testplans.ctia.org

Acknowledgements

Apple: Wisuit Sinsathitchai, Taeho Park, Indranil Sen

AT&T: Scott Prather

EMITE: Miguel Ángel García Fernández

ETS-Lindgren: Edwin Mendivil, Michael Foegelle

Keysight Technologies: Thorsten Hertel

MVG: Kim Rutkowski, Alessandro Scannavini

PCTEST Engineering Laboratory, LLC: Ron Borsato

Rohde & Schwarz: Jose M. Fortes

Sporton International: Lorien Chang, Will Ni, Alexander Ho

Verizon Wireless: Andrew Youtz

Table of Contents

List of Figures

List of Tables

Section 1 Introduction

1.1 Purpose

The purpose of this test plan is to define the CTIA Certification Program test requirements for performing Radiated RF Power and Receiver Performance measurements on wireless devices supporting frequency range 2 (FR2) in the EN-DC mode (using the LTE network).

1.2 Scope

This test plan defines general requirements for equipment configurations, laboratory techniques, test methodologies, and evaluation criteria that must be met in order to ensure the accurate, repeatable, and uniform testing of wireless devices supporting NR FR2 in EN-DC mode to ensure that they meet CTIA Certification standards. This test plan also defines a portion of the requirements that a laboratory must satisfy to qualify for and maintain CTIA Authorized Testing Laboratory (CATL) status (contact the CTIA Certification Program staff for complete CATL requirements).

This test plan does not provide specific test equipment configurations or detailed test instructions by which to execute certification testing. Such documentation and procedures must be presented by the CATL as part of the CTIA authorization process and subsequently maintained and employed by the CATL to remain authorized to perform Certification testing.

1.3 Reference Documents

The following documents are referenced in this Test Plan. For undated references, the latest edition of the referenced document applies. For dated references, only the edition cited applies. In the case where the same reference is dated and undated, the specific reference to the document in the test plan shall be considered to determine if the dated or undated version is to be used.

[1] *Guide to the Expression of Uncertainty in Measurement*, Genèva, Switzerland, International Organization for Standardization, 1995.

[2] *CTIA Test Plan for Wireless Device Over-the-Air Performance*; *Method of Measurement for Radiated RF Power and Receiver Performance*

[3] J. J. Thomson, *On the Structure of the Atom*, Phil. Mag., 7, 237 - 265, 1904

[4] https://www.mathworks.com/matlabcentral/fileexchange/37004-suite-of-functions-to-perform-uniform-sampling-of-a-sphere

[5] C. W. Clenshaw and A. R. Curtis, *A Method for Numerical Integration on an Automatic Computer*, Numerische Mathematik 2, p. 197-205, 1960

[6] P. J. Davis and P. Rabinowitz, *Methods of Numerical Integration*, Academic Press Inc., San Diego, 1984

[7] http://people.sc.fsu.edu/~jburkardt/m_src/clenshaw_curtis_rule/clenshaw_curtis_rule.html

[8] Georgy Voronoi, *Nouvelles Applications des Paramètres Continus à la Théorie des Formes Quadratiques*. Journal für die Reine und Angewandte Mathematik. 1908 (133): 97-178

[9] 3GPP TS 38.509: *Special Conformance Testing Functions for User Equipment (UE)*

[10] 3GPP TS 38.521-3: *User Equipment (UE) Conformance Specification; Radio Transmission and Reception*; Part 3: Range 1 and Range 2 Interworking operation with other radios

[11] 3GPP TS 38.521-2: *User Equipment (UE) Conformance Specification*; *Radio Transmission and Reception;* Part 2: Range 2 Standalone

[12] 3GPP TS 38.508-1: *User Equipment (UE) Conformance Specification*; Part 1: Common test environment

1.4 Acronyms and Definitions

The following specialized terms and acronyms are used throughout this document.

Table 1.4-1 Acronyms and Definitions

Acronym	Definition
AUT	Antenna Under Test
Beam correspondence	The ability of the UE to select a suitable beam for UL transmission based on DL measurements with or without relying on UL beam sweeping
BW	Bandwidth
CATR	Compact Antenna Test Range
CATL	CTIA Authorized Testing Laboratory
CCDF	Complementary Cumulative Distribution Function
CDF	Cumulative Distribution Function
D	DUT Radiating Aperture
DC	Dual Connectivity
DFT-s-OFDM	Discrete Fourier Transform-spread-OFDM
DUT	Device Under Test
EIRP	Effective Isotropic Radiated Power
EIS	Equivalent Isotropic Sensitivity
EN-DC	E-UTRA/NR DC
DUT	Device Under Test
FR1	Frequency Range 1
FR2	Frequency Range 2
MOP	Maximum Output Power

Acronym	Definition
MU	Measurement Uncertainty
NR	New Radio
OFDM	Orthogonal Frequency-Division Multiplexing
OTA	Over The Air
PDF	Probability Density Function
Pol_{Link}	Polarization, either θ or ϕ, of the DL signal transmitted by the test equipment through the measurement antenna for the DUT to form the TX/RX beam towards it
Pol_{Meas}	Polarization, either θ or ϕ, of the measurement antenna of the test equipment for the measurement being performed
REFSENS	Reference Sensitivity
RF	Radio Frequency
RX	Receiver
RX beam peak direction	Direction (θ,ϕ) where the best receiver performance is found
SCS	Sub-Carrier Spacing
Test System	The controlled propagation environment used for evaluation of the Device Under Test (DUT). In the context of this version of this test specification, the Compact Antenna Test Range (CATR) is the only valid test system
Test Methodology	The process used to execute tests against the DUT using the Test System(s) specified by this document. In the context of this version of this test specification, the Indirect Far Field methodology based on Compact Antenna Test Range (CATR) is the only permitted test methodology
TRP	Total Radiated Power
TX	Transmitter
TX beam peak direction	Direction (θ,ϕ) where the maximum total component of EIRP is found
Quiet Zone	The portion of the useable volume within the test system into which the DUT can be placed and in which the test criteria are met within the applicable uncertainty limits
QoQZ	Quality of Quiet Zone
QZ	Quiet Zone
UBF	UE Beamlock test Function
UE	User Equipment

Acronym	Definition
θ	Denotes the zenith angle (in degrees) within the spherical co-ordinate system, as well as measurement antenna polarization along the direction of motion of the zenith axis rotation
ϕ	Denotes the azimuth angle (in degrees) within the spherical co-ordinate system, as well as measurement antenna polarization along the direction of motion of the azimuth axis rotation

1.5 5G Millimeter-Wave Test Overview

This test plan presents the individual test procedures organized by type of test (Transmitter, Receiver).

The testing requirements fall into 4 categories:

- Measuring the basic performance of the test chamber
- Measuring the path loss of the test system
- Measuring the TX and RX beam peak direction
- Measuring the TX and RX performance of the wireless device

The test methodologies permitted for evaluating the TX and RX performance as part of the CTIA Certification program are introduced in Section 2. The basic performance of the test chamber is covered in Section 3 and includes a site validation method used to determine the uncertainty contribution of the test system. This quality of quiet zone validation shall be performed by every CATL initially as part of the CATL authorization process. Corrections for the path loss of the test system, including range length, measurement antenna, cables, amplifiers, etc. are determined using the range reference measurement described in Section 4. The measurement of the wireless device is covered in Section 5 for radiated power measurements and Section 6 for sensitivity measurements. The respective beam peak search procedures to determine the directions towards which the DUT forms the TX/RX beams are included in Section 5 and Section 6. The overall measurement uncertainty is calculated in the manner described in Section 7 (using Appendix C as a guide).

1.6 Device under Test (DUT) and Accessories - The Wireless Device

See Section 1.5 of the CTIA OTA test plan [2]. No samples for conducted testing are required for this test plan. The UE's antennas shall not be configured or enabled/disabled in a manner that is contrary to the normal operation of the UE. The UE can, however, also be pre-configured by disabling UL TX diversity schemes similar to what 3GPP is currently mandating for conformance testing [11].

This test plan is currently applicable only to UE antennas with radiating aperture less than or equal to 5 cm. Measurement grids and measurement uncertainties for DUTs with antenna apertures greater than 5 cm have not been defined yet and can therefore not be certified using this test plan.

1.7 Wireless Device Documentation

See Section 1.6 of the CTIA OTA test plan [2].The reporting tables are listed in Appendix E.

To allow for test time reduction with the beam peak search measurements, the manufacturer is allowed to declare that the beam peak at the mid test frequency range is applicable for the remaining (low, high) test frequency ranges. Beam peak search results cannot be re-used across different bands.

Section 2 Permitted Test Methods

This section is outlining the permitted OTA test methods suitable for the UE OTA performance test cases outlined in this test plan.

2.1 Applicability Criteria

Note (Working Assumption): For Version 1.0.x of the test plan, only the Indirect Far-Field (IFF) based on Compact Antenna Test Range (CATR) methodology is considered a permitted method.

2.2 Equivalence Criteria

Note (Working Assumption): For Version 1.0.x of the test plan, only the Indirect Far-Field (IFF) based on Compact Antenna Test Range (CATR) methodology is considered a permitted method.

2.3 Direct Far-Field (DFF)

Note (Working Assumption): For Version 1.0.x of the test plan, only the Indirect Far-Field (IFF) based on Compact Antenna Test Range (CATR) methodology is considered a permitted method.

2.4 Indirect Far-Field (IFF) based on Compact Antenna Test Range (CATR)

2.4.1 Description

The IFF method utilizing a compact antenna test range (CATR) creates a far-field environment in relatively close proximity of the parabolic reflector which serves as collimator transforming spherical waves into plane waves within the desired quiet zone. Figure 2.4-1 and Figure 2.4-2 demonstrate the reciprocity of the CATR system concept.

For RX testing, as illustrated in Figure 2.4-1, the probe/feed antenna placed near the focal point of the reflector radiates a spherical wave towards the reflector which collimates it into a planar wave front received by the DUT. The focal length is approximately the distance between the feed and the reflector. On the other hand, for TX testing, as illustrated in Figure 2.4-2, the radiation pattern from the DUT can be described as a series of plane waves propagating in different directions and the probe/ feed antenna receives only the focused beam from the plane wave directed straight at the reflector.

Inside the quiet zone, a planar wave front (uniform amplitude and phase) is achieved. Amplitude uniformity is dependent on the feed pattern, feed alignment, and reflector design while phase planarity is mainly dependent on feed alignment and reflector design. The polarization purity is mainly dependent on the parabolic system geometry considering high polarization purity feeds.

Figure 2.4-1 Working Principle for Rx Testing in a CATR

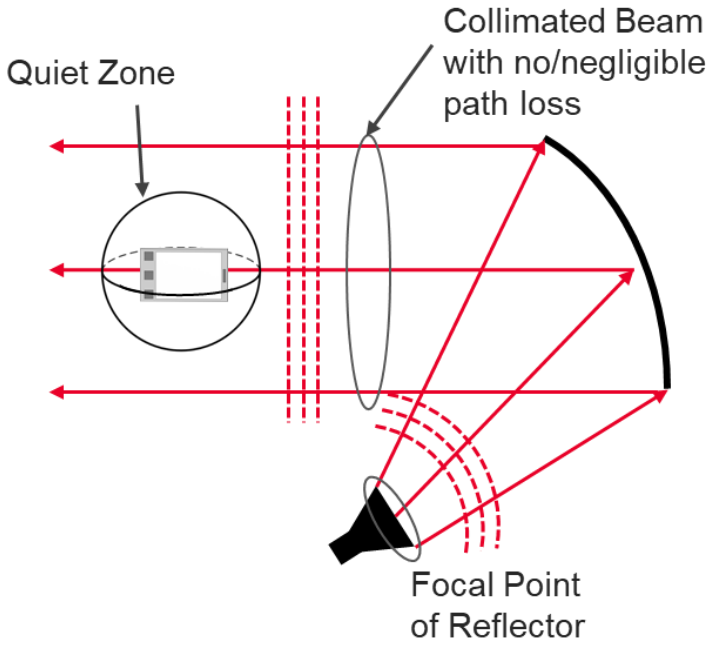

Figure 2.4-2 Working Principle for Tx Testing in a CATR

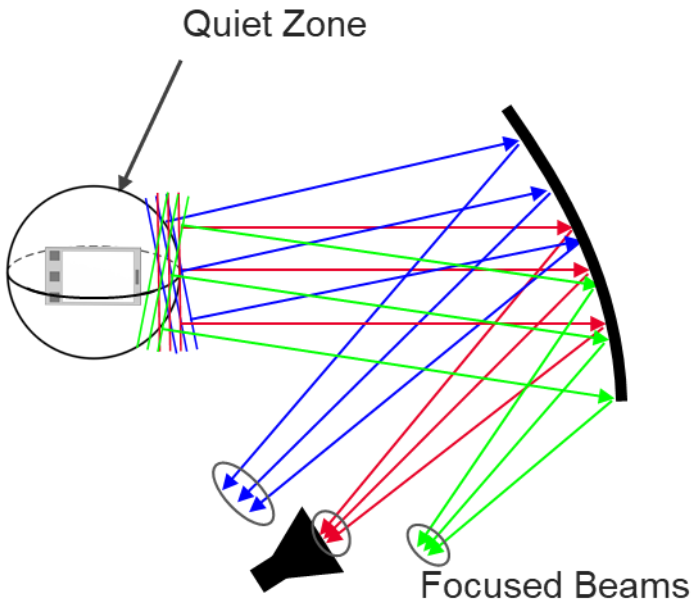

The key aspects of this test method setup are:

- A positioning system such that the angle between the dual-polarized measurement antenna and the DUT has at least two axes of freedom and maintains a polarization reference.

- Before performing the UE Beamlock test Function (UBF) identified in 3GPP TS 38.509 [9], the measurement probe acts as a link antenna maintaining polarization reference with respect to the DUT. Once the beam is locked, the link may be passed to the link antenna which maintains reliable signal level with respect to the DUT.

- For setups intended for measurements of UE RF characteristics in EN-DC mode with one UL configuration, an LTE link antenna is used to provide the LTE link to the DUT. The LTE link antenna provides a stable LTE signal without precise path loss or polarization control.

- For setups intended for measurements in NR CA mode with FR1 and FR2 inter-band NR CA, test setup provides NR FR1 link to the DUT. The NR FR1 link has a stable and noise-free signal without precise path loss or polarization control.

2.4.2 CATR Coordinate System

The IFF CATR measurement setup for FR2 is shown in Figure 2.4-3. The relative orientation of the coordinate system with respect to the reflector and the axes of rotation apply to any CATR measurement setup.

Figure 2.4-3 Example of IFF: CATR Measurement Setup

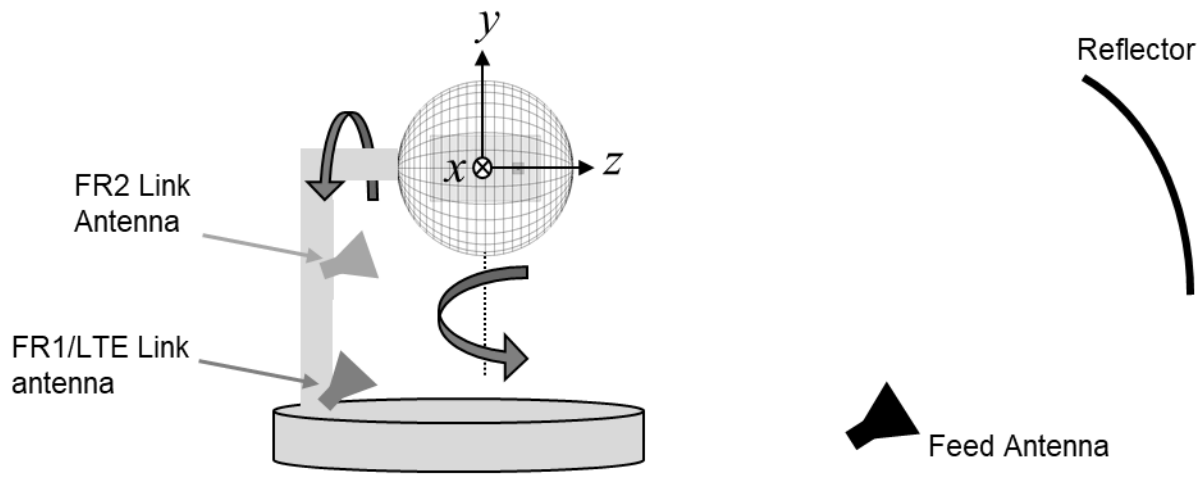

2.4.3 Quiet Zone (QZ) Dimension

The quiet zone shall be large enough to fully contain the DUT. The spherical quiet zone shall have a radius of 15 cm to accommodate smartphone UEs, CPEs, and small handheld DUTs. The device types are listed as examples and other device types are not precluded. In either case, the DUT shall be fully contained in one of the quiet zone sizes defined herein for the entire duration of the test.

2.4.4 Quality of the Quiet Zone (QoQZ)

The Quality of the Quiet Zone shall be measured for the frequencies defined in Section 3.3. The measured Quality of the Quiet Zone performance is used in uncertainty calculations for the appropriate Quality of the Quiet Zone dimension utilized for the DUT.

2.4.5 Measurement Distance

The CATR system does not require a measurement distance of $R > 2D^2/\lambda$ to achieve a plane wave as in a conventional anechoic chamber test methodology (direct far-field). Instead, for the CATR system, the far-field distance is seen as the focal length.

The measurement distance for any CATR system implementation shall be adequate to meet the quiet zone dimensions defined in Section 2.4.3.

As the CATR generates a plane wave with no free space path loss inside the quiet zone, the influence of measurement distance on measurement uncertainty can be considered as zero as defined in Appendix C.3.

2.5 Near-Field-to-Far-Field Transform (NFTF)

Note (Working Assumption): For Version 1.0.x of the test plan, only the Indirect Far-Field (IFF) based on Compact Antenna Test Range (CATR) methodology is considered a permitted method.

Section 3 Test Site Characteristics and Quiet Zone Accuracy

3.1 Minimum Measurement Distance

The quality of quiet zone validation shall be performed in the far-field of the UE antennas.

3.2 Equipment Required

The reference Antenna Under Test (AUT) that is placed at various locations within the quiet zone shall be a directive antenna with similar properties of typical antenna arrays integrated in DUTs. The required characteristics in terms of Directivity and Half Power Beamwidth (HPBW) of the reference AUT are shown in Figure 3.2-1, Figure 3.2-2 and Figure 3.2-3.

Figure 3.2-1 Directivity Mask

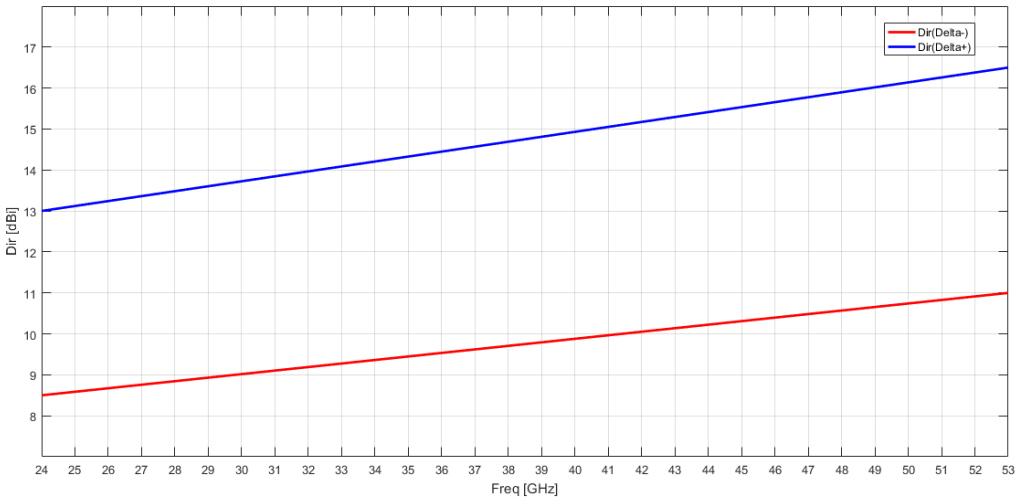

Figure 3.2-2 HPBW-E mask

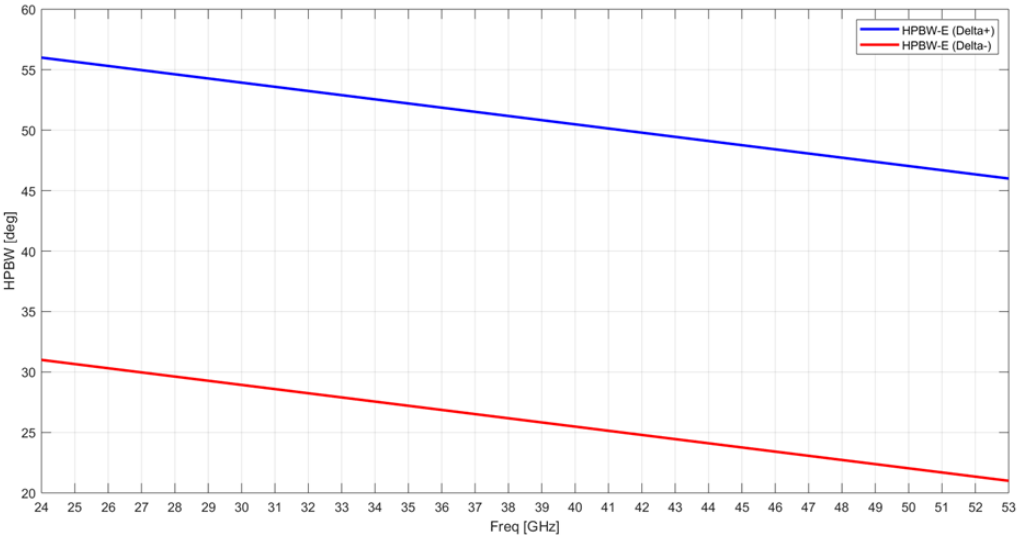

Figure 3.2-3 HPBW-H mask

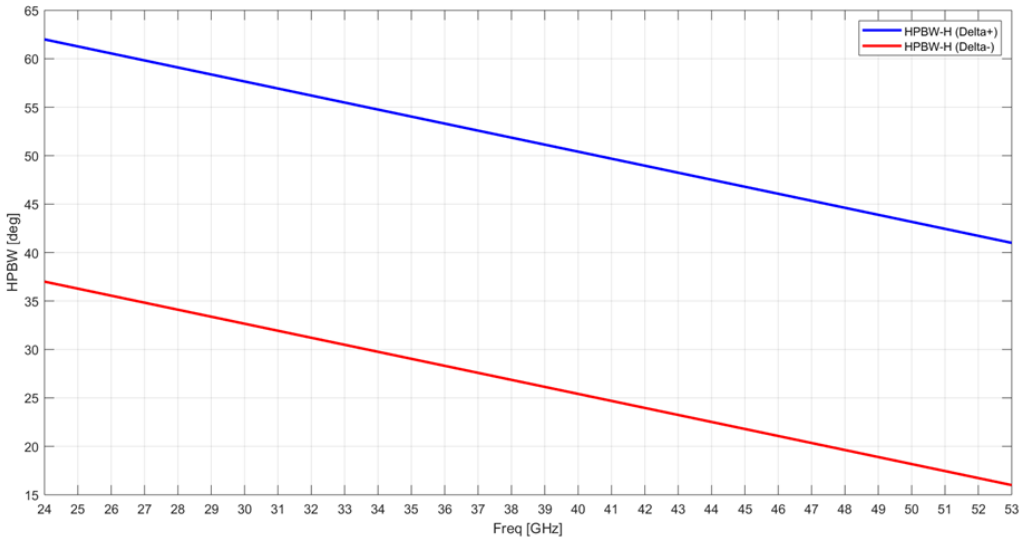

The AUT shall be symmetric on E and H planes.

The above masks for the reference antenna are met based on antenna vendors' calibration report or measurements performed by the lab.

For the measurement, a combination of signal generator and spectrum analyzer or a network analyzer can be used. The multi-port (with at least three ports) network analyzer is most suitable to reduce test time as both polarizations of the measurement antenna can be measured simultaneously, and multiple frequencies can be measured within a sweep.

3.3 Test Frequencies

The FR2 frequency range from 24250 to 52600 MHz is split up into four different ranges, referred to as FR2_1 through FR2_4, as outlined in Table 3.3-1, to limit the number of test frequencies to a manageable number. Defining test frequencies per operating band would likely increase to an impractical number as additional operating bands are defined. The Quality of Quiet Zone is determined at two test frequencies per frequency range and the maximum Quality of Quiet Zone measurement at either of these two frequencies would be applied to the MU budget for the respective frequency range, e.g., QoQZ (FR2_1) = max (QoQZ($FR2\_1_{min}$), QoQZ($FR2\_1_{max}$)).

Table 3.3-1 QoQZ Test Frequencies

Designation	Operating Bands Covered	QoQZ Test Frequencies	
		Min [MHz]	Max [MHz]
FR2_1	n257, n258, n261	24250	32000
FR2_2	n260	32000	40000
FR2_3		40000	48000
FR2_4		48000	52600

3.4 Quality of Quiet Zone Measurement Procedure

This procedure describes the procedures for validating the Quality of the Quiet Zone for the permitted far-field methodologies. This procedure is mandatory before the test system is commissioned for certification tests and characterizes the quiet zone performance of the anechoic chamber, specifically the effect of reflections within the anechoic chamber including any positioners and support structures. Additionally, it includes the effect of offsetting the directive antenna array inside a DUT from the center of the quiet zone, i.e., the center of rotation of the DUT and measurement antenna positioning systems as well as the directivity MU, i.e., the variation of antenna gains in the different direct line-of-sight links.

The spherical quiet zone is illustrated in Figure 3.4-1, which includes the definitions of center of quiet zone location, i.e., the geometric center of the positioning systems and the size, i.e., radius *R*.

Figure 3.4-1 Quiet Zone Illustration

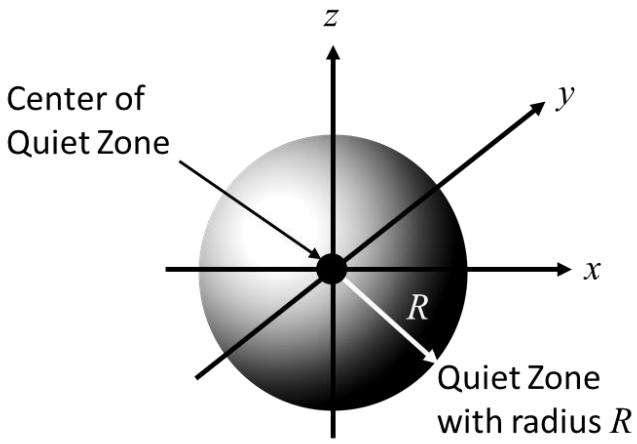

The outcome of the procedures can be used to estimate the following:

- variation of the TRP measurements, spherical surface integrals of EIRP when the DUT is placed anywhere within the quiet zone and with the beam formed in any arbitrary direction inside the chamber

- variation of the EIRP/EIS measurements when the DUT is placed anywhere within the quiet zone and with the beam formed in any arbitrary direction inside the chamber

The reference coordinate system defined in Appendix A.1 applies to this procedure.

The Quality of the Quiet Zone measurements for integrated RF parameters such as TRP shall use 3D pattern measurements of the reference antenna patterns as they most closely resemble the 3D/spherical surface measurements/integrals of EIRP or EIS. Therefore, the Quality of the Quiet Zone measurements for TRP metrics shall be based on efficiency measurements. On the other hand, the Quality of the Quiet Zone measurements for single-directional EIRP and EIS metrics shall be based on gain measurements of the direct line-of-sight link between the reference AUT and the measurement antenna.

3.5 Reference AUT Orientations and Coordinate Systems

The reference AUT shall be positioned in a total of 7 different reference positions, shown in Figure 3.5-1.

Figure 3.5-1 Reference AUT Positions

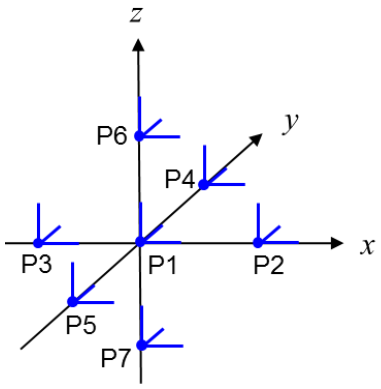

While position 1, P1, is the center of the quiet zone, the remaining positions, 2 through 7, are off-center positions each displaced by the radius of the quiet zone, *R*. The coordinates of the respective test points are shown in Table 3.5-1.

Table 3.5-1 Reference AUT Measurement Coordinates

Position	X	Y	Z
P1	0	0	0
P2	*R*	0	0
P3	*-R*	0	0
P4	0	*R*	0
P5	0	*-R*	0
P6	0	0	*R*
P7	0	0	*-R*

Due to the non-commutative nature of rotations, the order of rotations is important and needs to be defined when reference AUT orientations are tested. The reference orientation of the reference AUT is shown in Figure 3.5-2.

Figure 3.5-2 Illustration of Reference AUT Orientation

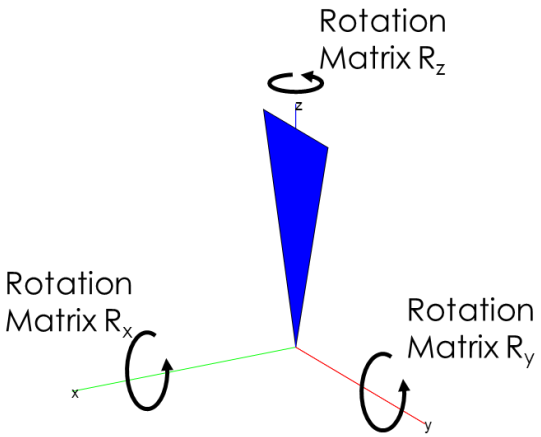

The rotations around the x, y, and z axes can be defined with the following rotation matrices:

$$R_x(\alpha) = \begin{bmatrix} 1 & 0 & 0 & 0 \\ 0 & \cos\alpha & -\sin\alpha & 0 \\ 0 & \sin\alpha & \cos\alpha & 0 \\ 0 & 0 & 0 & 1 \end{bmatrix}$$

$$R_y(\beta) = \begin{bmatrix} \cos\beta & 0 & \sin\beta & 0 \\ 0 & 1 & 0 & 0 \\ -\sin\beta & 0 & \cos\beta & 0 \\ 0 & 0 & 0 & 1 \end{bmatrix}$$

And:

$$R_z(\gamma) = \begin{bmatrix} \cos\gamma & -\sin\gamma & 0 & 0 \\ \sin\gamma & \cos\gamma & 0 & 0 \\ 0 & 0 & 1 & 0 \\ 0 & 0 & 0 & 1 \end{bmatrix}.$$

with the respective angles of rotation, α, β, γ and:

$$\begin{bmatrix} x' \\ y' \\ z' \\ 1 \end{bmatrix} = R \begin{bmatrix} x \\ y \\ z \\ 1 \end{bmatrix}$$

Additionally, any translation of the reference AUT can be defined with the translation matrix:

$$T(t_x, t_y, t_z) = \begin{bmatrix} 1 & 0 & 0 & t_x \\ 0 & 1 & 0 & t_y \\ 0 & 0 & 1 & t_z \\ 0 & 0 & 0 & 1 \end{bmatrix}$$

with offsets t_x, t_y, t_z in x, y, and z, respectively and with:

$$\begin{bmatrix} x' \\ y' \\ z' \\ 1 \end{bmatrix} = T \begin{bmatrix} x \\ y \\ z \\ 1 \end{bmatrix}$$

The combination of rotations and translation is captured by the multiplication of rotation and translation matrices.

For instance, the matrix M:

$$M = T(t_x, t_y, t_z) \cdot R_x(\alpha) \cdot R_y(\beta) \cdot R_z(\gamma)$$

describes an initial rotation of the DUT around the z axis with angle γ, a subsequent rotation around the y axis with angle β, and a final rotation around the x axis with angle α. After those rotations, the DUT is translated by t_x, t_y, t_z in x, y, and z, respectively.

3.5.1 Distributed-axes System

The reference AUT positions inside a typical distributed-axes system are shown in Figure 3.5-3.

Figure 3.5-3 Reference AUT Measurement Positions for Distributed-Axes System

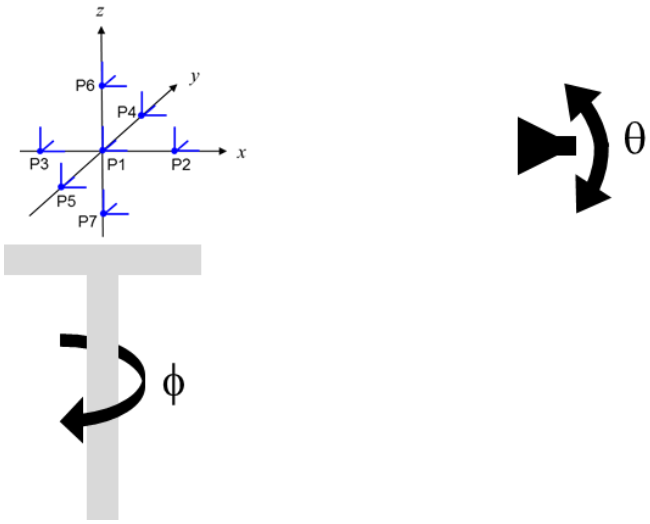

As different areas within the chamber could yield variations in the field uniformity inside the quiet zone caused by reflections, it is important to characterize the electromagnetic fields with the reference antennas uniformly illuminating the anechoic chamber.

In order to keep the Quality of the Quiet Zone characterization manageable in terms of test times, it is suggested to perform the reference measurements for the reference AUT placed at the 7 antenna positions with the antenna rotated around the y axis with 5 different angles β, i.e., β = 0°, 45°, 90°, 135°, and 180°, and rotated around the z axis with 8 different γ = 0°, 45°, 90°, 135°, 180°, 225°, 270°, and 315°. A graphical illustration of some sample reference AUT orientations is shown in Figure 3.5-4 for the reference AUT placed at position 6, P6, for reference antenna polarization γ_{pol} = 0° (illustrated in blue) and for the reference polarization γ_{pol} = 90° (illustrated in red).

The matrix operation for the rotations and translation is defined as:

$$M = T(t_x, t_y, t_z) \cdot R_z(\gamma) \cdot R_y(\beta) \cdot R_{z,pol}(\gamma_{pol})$$

for the distributed-axes system.

Figure 3.5-4 Sample reference AUT orientations for position 6, P6 for reference antenna polarizations γ_{pol} = 0° and γ_{pol} = 90°

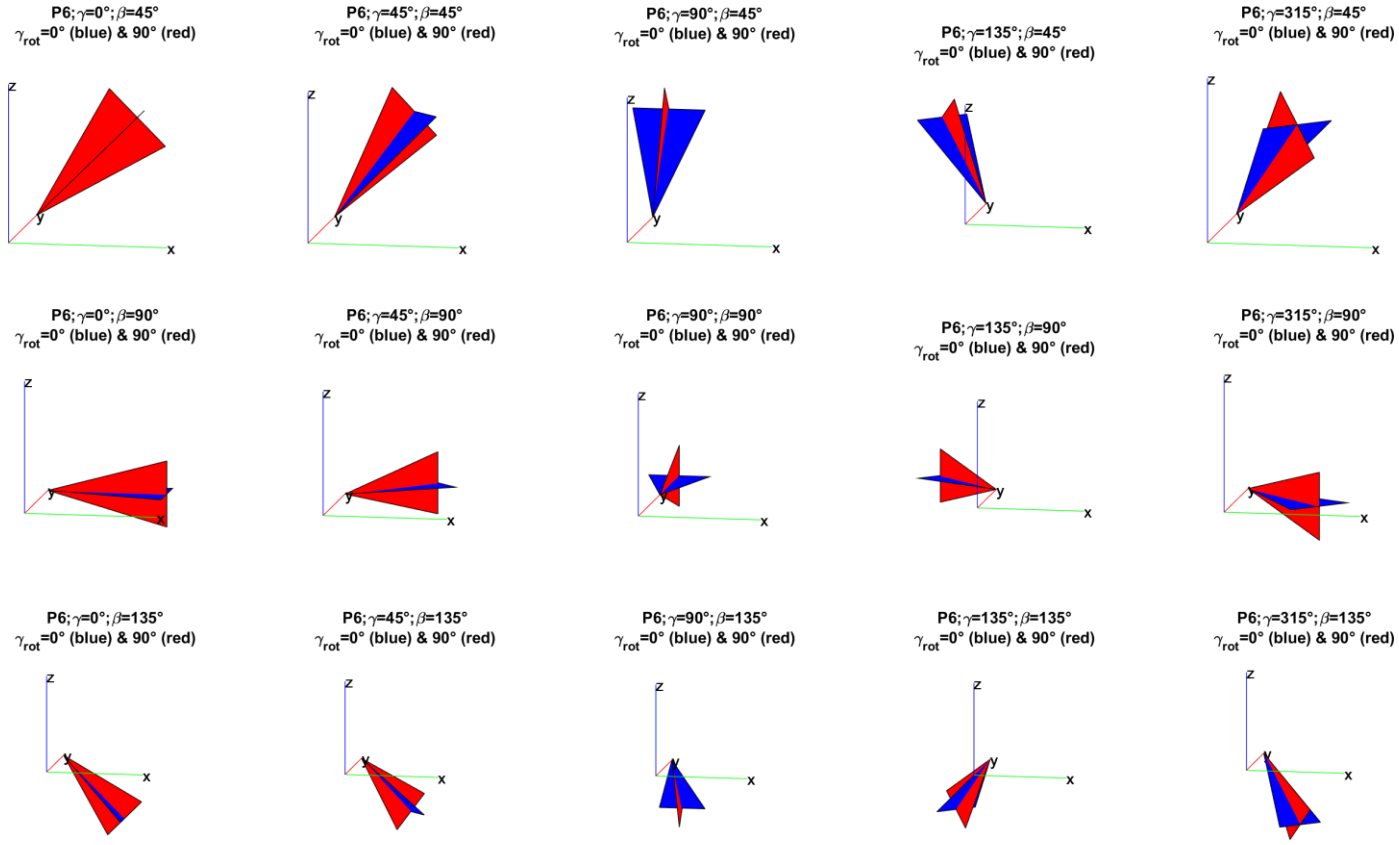

When facing the z-axis (along the turntable axis), β= 0° and β = 180°, the antenna does not need to be evaluated for the 8 different rotations around the z axis. A single roll orientation is sufficient since those orientations are unique. Due to the pedestal, distributed-axes systems are not able to measure towards the β = 180° direction; for those systems, the reference measurements at this reference AUT orientation can be skipped.

If the device re-positioning approach outlined in Appendix A.1 is adopted for the EIRP/EIS/TRP based conformance test cases, the quality of quiet zone analysis is sufficient only for γ = 0°, 45°, 90°.

3.5.2 Combined-axes System

The reference AUT positions inside a typical combined-axes system are shown in Figure 3.5-5.

Figure 3.5-5 Reference AUT Measurement Positions for combined-axes System

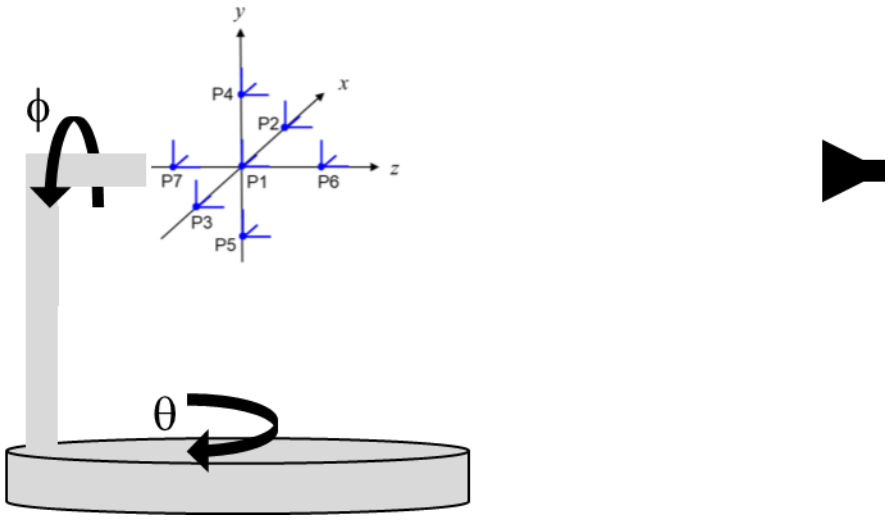

In order to keep the Quality of the Quiet Zone characterization manageable in terms of test times, it is suggested to perform the reference measurements for the reference AUT placed at the 7 antenna positions with the antenna rotated around the x axis with 5 different angles α, i.e., α = -90°, -45°, 0°, 45°, and 90° and rotated around the y axis with 8 different angles β = 0°, 45°, 90°, 135°, 180°, 225°, 270°, and 315°. A graphical illustration of some sample reference AUT orientations is shown in Figure 3.5-6 with a reference AUT placed at position 4, P4, for the reference polarizations γ_{pol} = 0° (illustrated in blue) and γ_{pol} = 90° (illustrated in red).

The matrix operation for the rotations and translation is defined as

$$M = T(t_x, t_y, t_z) \cdot R_y(\beta) \cdot R_x(\alpha) \cdot R_{z,pol}(\gamma_{pol})$$

for the combined-axes system.

Figure 3.5-6 Sample reference AUT orientations for position 4, P4, for reference antenna polarization γ_{pol} = 0° and γ_{pol} = 90°.

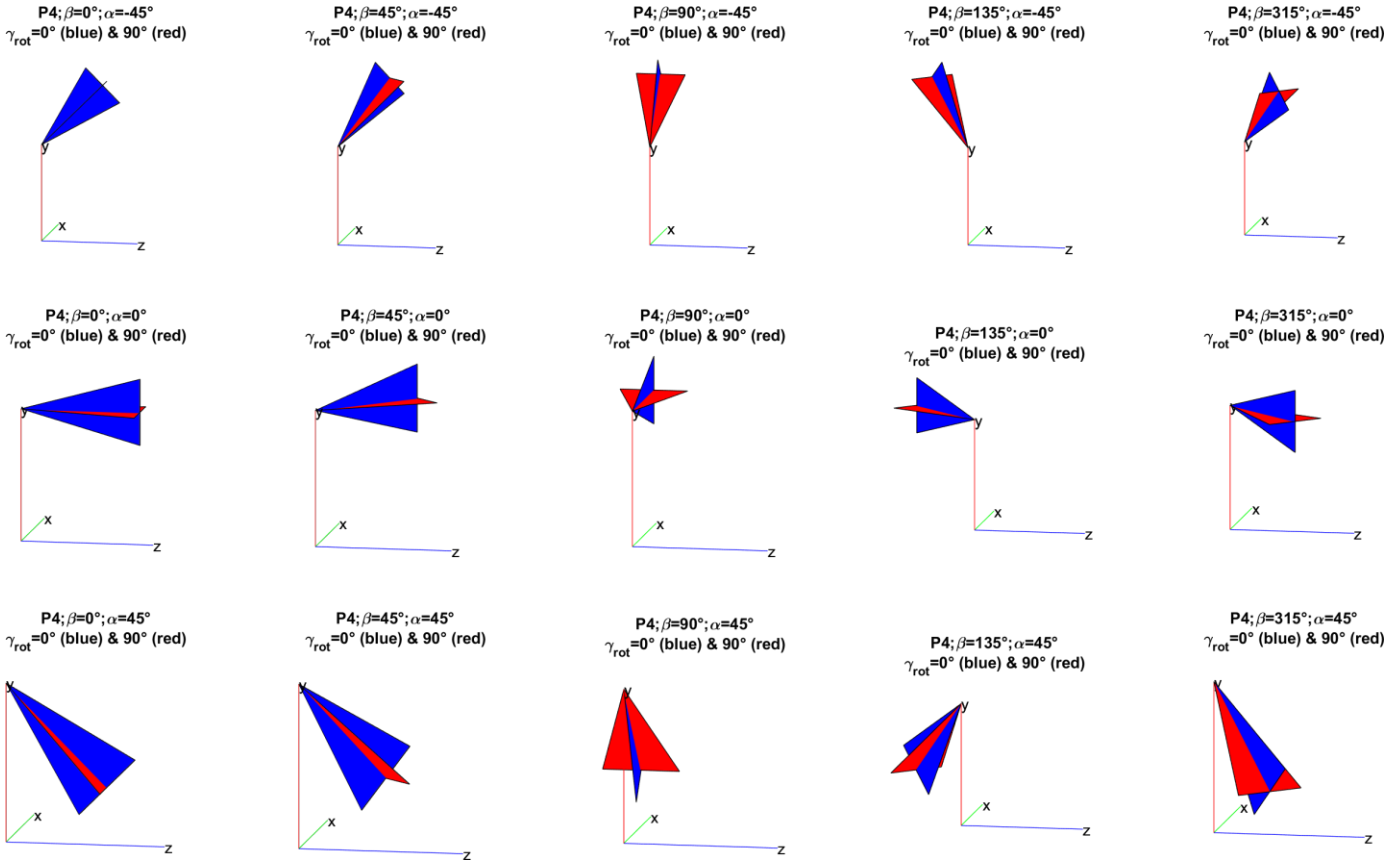

When facing the y axis (along the turntable axis), α = 90° and α = -90°, the antenna does not need to be evaluated for the 8 different rotations around the y axis. A single rotation is sufficient since those orientations are unique. Due to the pedestal of the 2-axis positioner, combined-axes systems are not able to measure towards the β = 180° direction; for those systems, the reference measurements at this reference AUT orientation can be skipped.

If the device re-positioning approach outlined in Appendix A.1 is adopted for all EIRP/EIS/TRP based conformance test cases, the quality of quiet zone analysis is sufficient only for β = 0°, 45°, 90°, 270°, and 315°.

3.6 Statistical Analysis

The combined MU element related to the Quality of the Quiet Zone for TRP and the offset between the UE's antenna array and center of the quiet zone is the standard deviation of the various efficiency measurement results that are based on the 7 different reference AUT positions, the respective reference AUT orientations, and the two reference AUT polarization orientations.

The combined MU element related to the Quality of the Quiet Zone for EIRP/EIS, offset between UE antenna array and center of quiet zone, and directivity is the standard deviation of the single-point gain measurement results that are based on the 7 different reference AUT positions, the respective reference AUT orientations, and the two reference AUT polarization orientations.

Section 4 Range Reference Requirements

This section describes the required procedure for obtaining the reference measurement used in removing the test system's influence from the Radiated Power and Sensitivity measurements. Before accurate measurements of quantities such as TRP, EIRP, or EIS can be made, it is necessary to perform a reference measurement to account for the various factors affecting the measurement of these quantities. These factors include components like range length path loss, gain of the receive antenna, cable losses, and so forth. This reference measurement is performed using a reference antenna (typically a standard gain horn) with known gain characteristics. The reference antenna is mounted at the center of the quiet zone to serve as the substitute Antenna Under Test (AUT). The reference measurement is repeated for each variation of the measurement system (i.e., each polarization of the receive antenna, and each possible signal path to the measurement equipment). The reference measurement is combined with the gain of the reference antenna to determine an isotropic reference correction to be applied to DUT measurements performed using the test system. This procedure shall be repeated regularly and any time there is a change in the measurement system that may affect the validity of this reference measurement. It is recommended to perform this procedure on a monthly or quarterly basis to determine system stability.

4.1 Theoretical Background

See Section 1.5 of the CTIA OTA test plan [2].

4.2 Equipment Required

See Section 1.6 of the CTIA OTA test plan [2]. Reference antennas in the mm-wave frequency range are typically directive horn antennas. A single broadband or multiple standard horn antennas can be used to cover the different frequency ranges of interest.

4.3 Test Frequencies

Table 4.3-1 provides the minimum list of reference frequencies to be measured. Additional points should be taken to cover each expected DUT test frequency. A swept spectrum reference measurement is recommended; the exact frequencies in Table 4.3-1 are not required as long as the frequency resolution is sufficient enough to ensure that there are no sharp resonances in the measurement system near the required test frequencies.

Table 4.3-1 Test Frequencies for the Reference Measurement

Band	Range	Frequency [MHz]
3GPP Band n260	UL&DL Low	37051.80
	UL&DL Mid	38498.88
	UL&DL High	39949.92
3GPP Band n261	UL&DL Low	27559.32
	UL&DL Mid	27923.52
	UL&DL High	28292.16

4.4 Test Procedures

See Section 4.4 of the CTIA OTA test plan [2].

Section 5 Test Procedures – Transmitter

This section outlines the test procedures for the transmitter test cases for this test plan.

For the test environmental conditions described in [11], only the normal conditions shall be applied, i.e., normal temperature and normal voltage.

The vendor shall submit to the CATL a declaration of the primary mechanical mode as referenced in this test plan. Device mechanical modes that are not representative of end use do not need to be tested. The CATL shall use the primary mechanical mode to test low, mid, and high frequency ranges and use these results when applying the pass/fail limits (if applicable). Testing in non-primary mechanical modes is only required in the low and high frequency ranges; mid frequency range testing is not required.

The TX procedures in this section shall assume that the DUT autonomously chooses the corresponding TX beam for PUSCH transmission using downlink reference signals to transmit in the direction of the incoming DL signal, which is based on beam correspondence without relying on UL beam sweeping.

5.1 TX Beam Peak Search Procedure

The purpose of this procedure is to determine the TX beam peak direction where the maximum total component of EIRP is found.

The measurement system shall be configured as specified in Section 2. The power radiated by the DUT in the FR2 measurement path shall be measured using a calibrated RF measuring instrument, e.g., a gNB emulator, spectrum analyzer, or power meter capable of averaging across at least one subframe (1ms).

Using the settings in Clause 6.2B.1.4.1.4 of TS 38.521-3 [10], establish the LTE and NR FR2 connections.

Instead of the NR test conditions defined in Clause 6.2.1.1.4.1 [11], TX test cases shall be executed for the three test frequency ranges using:

- One modulation scheme
- One operating bandwidth
- One SCS, and
- Inner Full RB allocations across the bands supported by the DUT, as defined in Table 5.1-1.

The TX beam peak search shall be performed for each of the test frequency ranges defined in Table 5.1-1 unless the device manufacturer declares that the TX beam peak direction from the mid test frequency range can be re-used for the low and high test frequency ranges. Beam peak search results cannot be re-used across different bands that are not overlapping. The report must clearly state that the beam peak directions for the low and high frequency ranges have not been determined with a beam peak search procedure but instead have re-used beam peak directions per the DUT vendor declaration.

Table 5.1-1 Test Conditions for NR Operating Bands n260 and n261

Band	Bandwidth [MHz]	SCS [kHz]	Range	Modulation	UL RB Allocation (Inner Full)	DI Config.	Center Frequency of Carrier [MHz]	RF Channel Number [ARFCN]
n260	100	120	UL&DL Low	DFT-s-OFDM QPSK	20@22	N/A	37051.80	2230029
			UL&DL Mid				38498.88	2254147
			UL&DL High				39949.92	2278331
n261	100	120	UL&DL Low	DFT-s-OFDM QPSK	20@22	N/A	27559.32	2071821
			UL&DL Mid				27923.52	2077891
			UL&DL High				28292.16	2084035

The minimum number of measurement grid points for the TX beam peak search are outlined in Appendix D.3.

The TX beam peak procedure is defined as follows:

1. Select any of the three Alignment Options (1, 2, or 3) from Table A.1-1 through Table A.1-3 to mount the DUT inside the QZ.
2. Position the DUT in DUT Orientation 1 from Table A.1-1 through Table A.1-3,
3. Connect the SS (System Simulator) with the DUT through the reference measurement antenna with $Pol_{Link}=\theta$ polarization to form the TX beam towards the measurement antenna. Allow at least BEAM_SELECT_WAIT_TIME (defined in Annex K.1.1 of TS 38.521-2 [11]) for the UE TX beam selection to complete. Continuously send power control "up" commands in every uplink scheduling information to the UE; allow at least 200 ms after the first TPC command in this step to ensure that the UE transmits at its maximum output power before continuing.
    a. SS activates the UE Beamlock Function (UBF) by performing the procedure as specified in TS 38.508-1 [12] Clause 4.9.2 using condition TX only
    b. Measure the mean power P_{meas} ($Pol_{Meas}=\theta$, Pol_{Link}) of the modulated signal arriving at the power measurement equipment
    c. Calculate EIRP ($Pol_{Meas}=\theta$, Pol_{Link}) by adding the composite loss of the entire transmission path for utilized signal path, $L_{EIRP,\theta}$, and frequency to the measured power $P_{meas}(Pol_{Meas}=\theta, Pol_{Link})$.
    d. Measure the mean power P_{meas} ($Pol_{Meas}=\phi$, Pol_{Link}) of the modulated signal arriving at the power measurement equipment.

e. Calculate EIRP ($Pol_{Meas}=\phi$, Pol_{Link}) by adding the composite loss of the entire transmission path for utilized signal path, $L_{EIRP,\phi}$, and frequency to the measured power P_{meas} ($Pol_{Meas}=\phi$, Pol_{Link}).
f. Calculate total EIRP($Pol_{Link}=\theta$) = EIRP($Pol_{Meas}=\theta$, Pol_{Link}) + EIRP($Pol_{Meas}=\phi$, Pol_{Link}).
g. SS deactivates the UE Beamlock Function (UBF) by performing the procedure as specified in TS 38.508-1 [12] Clause 4.9.3.

4. Connect the SS (System Simulator) with the DUT through the measurement antenna with $Pol_{Link}=\phi$ polarization to form the TX beam towards the measurement antenna. Allow at least BEAM_SELECT_WAIT_TIME for the UE TX beam selection to complete. Perform steps a-g from Step 3.
5. Advance to the next grid point and repeat steps 3 and 4 until measurements within zenith range $0^o \le \theta \le 90^o$ have been completed,
6. After the measurements within zenith range $0^o \le \theta \le 90^o$ have been completed and:
   a. if the re-positioning concept is applied to the TX test cases, position the device in DUT Orientation 2 (either Options 1 or 2) for the Alignment Option selected in Step 1. For the TX beam peak search in the second hemisphere, continue steps 3 and 4 for the range of zenith angles $90^o < \theta \le 0^o$.
   b. If the re-positioning concept is not applied to the TX test cases, continue steps 3 and 4 for the range of zenith angles $90^o < \theta \le 180^o$

The TX beam peak direction is where the maximum total component of EIRP($Pol_{Link}=\theta$) or EIRP($Pol_{Link}=\phi$) is found.

5.2 Maximum Output Power – EIRP

The intent of this test procedure is to measure the total component of the EIRP in the maximum TX beam peak direction found in Section 5.1. The test conditions defined in Table 5.1-1 apply for this test case.

The test procedure for maximum output power EIRP at the TX beam peak direction is defined as follows:

1. Select any of the three Alignment Options (1, 2, or 3) from Table A.1-1 through Table A.1-3 to mount the DUT inside the QZ.
2. If the re-positioning concept is not applied to the TX test cases, position the device in DUT Orientation 1. If the re-positioning concept is applied to the TX test cases,
   a. Position the device in DUT Orientation 1 from Table A.1-1 through Table A.1-3 if the maximum beam peak direction is within zenith angular range $0^o \le \theta \le 90^o$ for the alignment option selected in step 1.
   b. Position the device in DUT Orientation 2 (either Options 1 or 2) from Table A.1-1 through Table A.1-3 if the maximum beam peak direction is within zenith angular range $90^o < \theta \le 180^o$ for DUT Orientation 1 for the alignment option selected in step 1.
3. SS sends uplink scheduling information for each UL HARQ process via PDCCH DCI format [0_1] for C_RNTI to schedule the UL RMC according to Table 6.2.1.1.4.1-1 of TS 38.521-2 [11]. Since the UL has no payload and no loopback data to send, the UE sends uplink MAC padding bits on the UL RMC. Messages to configure the appropriate uplink modulation in clause 4.6 of TS 38.508-1 [12].

4. Continuously send uplink power control "up" commands in every uplink scheduling information to the UE; allow at least 200 ms starting from the first TPC command in this step to ensure that the UE transmits at its maximum output power before continuing.
5. Set the DUT in the TX beam peak direction found in Section 5.1.
    a. Connect the SS (System Simulator) with the DUT through the measurement antenna with polarization reference Pol_{Link} that yielded the maximum TX beam peak to form the TX beam towards the TX beam peak direction and respective polarization. Allow at least BEAM_SELECT_WAIT_TIME for the UE TX beam selection to complete.
    b. SS activates the UE Beamlock Function (UBF) by performing the procedure as specified in TS 38.508-1 [12] clause 4.9.2 using condition TX only.
    c. Measure the mean power P_{meas} (Pol_{Meas}=θ, Pol_{Link}) of the modulated signal arriving at the power measurement equipment (such as a spectrum analyzer, power meter, or gNB emulator).
    d. Calculate EIRP (Pol_{Meas}=θ, Pol_{Link}) by adding the composite loss of the entire transmission path for utilized signal path, $L_{EIRP,\theta}$, and frequency to the measured power P_{meas} (Pol_{Meas}=θ, Pol_{Link}).
    e. Measure the mean power P_{meas} (Pol_{Meas}=ϕ, Pol_{Link}) of the modulated signal arriving at the power measurement equipment.
    f. Calculate EIRP (Pol_{Meas}=ϕ, Pol_{Link}) by adding the composite loss of the entire transmission path for utilized signal path, $L_{EIRP\ \phi}$ and frequency to the measured power P_{meas} (Pol_{Meas}=ϕ, Pol_{Link})
6. Calculate the resulting total EIRP (Pol_{Link}) for the chosen Pol_{Link} of θ or ϕ as follows: EIRP (Pol_{Link}) = EIRP (Pol_{Meas}=θ, Pol_{Link}) + EIRP (Pol_{Meas}=ϕ, Pol_{Link})

5.3 Maximum Output Power – TRP

The intent of this test procedure is to measure total radiated power of the DUT with the UL beam formed in the maximum TX beam peak direction found in Section 5.1.

The minimum number of measurement grid points including allowances to skip measurements near the pole at θ=180° for the TRP measurement are outlined in Appendix D.2.

The EN-DC connections are established as outlined in Section 5.1. The test conditions defined in Table 5.1-1 apply for this test case. The test procedure for TRP is as follows:

1. Select any of the three Alignment Options (1, 2, or 3) from Table A.1-1 through Table A.1-3 to mount the DUT inside the QZ.
2. If the re-positioning concept is not applied to the TX test cases, position the device in DUT Orientation 1. If the re-positioning concept is applied to the TX test cases,
    a. position the device in DUT Orientation 1 from Table A.1-1 through Table A.1-3 if the maximum beam peak direction is within zenith angular range 0°≤θ≤90° for the alignment option selected in step 1.
    b. Position the device in DUT Orientation 2 (either Options 1 or 2) from Table A.1-1 through Table A.1-3 if the maximum beam peak direction is within zenith angular range 90°<θ≤180° for DUT Orientation 1 for the alignment option selected in step 1.

3. SS sends uplink scheduling information for each UL HARQ process via PDCCH DCI format [0_1] for C_RNTI to schedule the UL RMC according to Table 6.2.1.1.4.1-1 of TS 38.521-2 [11]. Since the UL has no payload and no loopback data to send, the UE sends uplink MAC padding bits on the UL RMC. Messages to configure the appropriate uplink modulation are defined in clause 4.6 of TS 38.508-1 [12].
4. Continuously send uplink power control "up" commands in every uplink scheduling information to the UE; allow at least 200 ms after the first TPC command in this step to ensure that the UE transmits at its maximum output power before continuing.
5. Set the DUT in the TX beam peak direction found in Section 5.1.
    a. Connect the SS with the DUT through the downlink antenna with desired polarization reference Pol_{Link} that yielded the maximum TX beam peak to form the TX beam towards the desired TX beam direction and respective polarization. Allow at least BEAM_SELECT_WAIT_TIME for the UE TX beam selection to complete.
    b. SS activates the UE Beamlock Function (UBF) for the entire duration of the test by performing the procedure as specified in TS 38.508-1 [12] clause 4.9.2 using condition TX only.
6. For each measurement point, measure P_{meas} ($Pol_{Meas}=\theta$, Pol_{Link}) and P_{meas} ($Pol_{Meas}=\phi$, Pol_{Link}).
7. Calculate EIRP ($Pol_{Meas}=\theta$, Pol_{Link}) and EIRP ($Pol_{Meas}=\phi$, Pol_{Link}) by adding the composite loss of the entire transmission path for utilized signal paths, $L_{EIRP,\theta}$, $L_{EIRP\phi}$ and frequency to the respective measured powers P_{meas}.
8. The TRP value for the measurement grid is calculated using the TRP integration approaches outlined in Appendix D.2.

5.4 Maximum Output Power – Spherical Coverage

The intent of this test procedure is to verify that the spatial coverage of the UE in expected directions is acceptable.

The test conditions defined in Table 5.1-1 apply for this test case.

The $EIRP_{50\%-CDF}$ is obtained from the Cumulative Distribution Function (CDF) computed using maximum(EIRP ($Pol_{Link}=\theta$), EIRP ($Pol_{Link}=\phi$)) for all grid points collected during the TX beam peak search in Section 5.1. Alternatively, the $EIRP_{50\%-CDF}$ can be obtained from the Cumulative Distribution Function (CDF) computed using maximum(EIRP ($Pol_{Link}=\theta$), EIRP ($Pol_{Link}=\phi$)) using the procedure outlined in Section 5.1 but for the minimum number of grid points outlined in Appendix D.4.

When using constant step size measurement grids, a theta-dependent correction shall be applied, i.e., the PDF probability contribution for each measurement point is scaled by the normalized Clenshaw-Curtis weights $W(\theta)/W(\theta=90^{o})$ as outlined in Appendix D.2.

Section 6 Test Procedure – Receiver

This section outlines the test procedures for the receiver test cases for this test plan.

For the test environmental conditions [11], only the normal conditions shall be applied, i.e., normal temperature and normal voltage.

The vendor shall submit a declaration of the primary mechanical mode as referenced in this test plan to the CATL. Device mechanical modes that are not representative of end use do not need to be tested. The CATL shall use the primary mechanical mode to test low, mid, and high frequency ranges and use these results when applying the pass/fail limits (if applicable). Testing in non-primary mechanical modes is only required in the low and high frequency ranges; mid frequency range testing is not required.

6.1 RX Beam Peak Search Procedure

The purpose of this procedure is to determine the RX beam peak direction where the minimum averaged EIS is found.

Using the settings in Clause 7.3B.2.4.4.1 of TS 38.521-3 [10], establish the LTE and NR FR2 connections.

Instead of the NR test conditions defined in Clause 7.3.2.4.1 [11], the RX test cases shall be carried out for the three test frequency ranges, one modulation, one bandwidth, one SCS, and Inner Full RB allocations across the bands supported by the DUT, as defined in Table 6.1-1.

The RX beam peak search shall be performed for each of the test frequency ranges defined in Table 6.1-1 unless the device manufacturer declares that the RX beam peak direction from the mid test frequency range can be re-used for the low and high test frequency ranges. Beam peak search results cannot be re-used across different bands that are not overlapping. The report must clearly state that the beam peak directions for the DUT's low and high frequency ranges have not been determined with a beam peak search procedure but have re-used the mid frequency direction per a DUT vendor declaration.

Table 6.1-1 Test Conditions for NR Operating Bands n260 and n261

Band	Bandwidth [MHz]	SCS [kHz]	Range	DL Modulation	DL Config.	UL Modulation	UL RB Allocation (Inner Full)	Center Frequency of Carrier [MHz]	RF Channel Number [ARFCN]
n260	100	120	UL&DL Low	CP-OFDM QPSK	Full (64@0)	DFT-s-OFDM QPSK	Full (64@0)	37051.80	2230029
			UL&DL Mid					38498.88	2254147
			UL&DL High					39949.92	2278331
n261	100	120	UL&DL Low	CP-OFDM QPSK	Full (64@0)	DFT-s-OFDM QPSK	Full (64@0)	27559.32	2071821
			UL&DL Mid					27923.52	2077891
			UL&DL High					28292.16	2084035

The minimum number of measurement grid points for the RX beam peak search are outlined in Appendix D.3.

The RX beam peak procedure is defined as follows:

1. Select any of the three Alignment Options (1, 2, or 3) from Table A.1-1 through Table A.1-3 to mount the DUT inside the QZ.
2. Position the DUT in DUT Orientation 1 from Table A.1-1 through Table A.1-3.
3. Connect the SS (System Simulator) with the DUT through the measurement antenna with $Pol_{Link}=\theta$ polarization to form the RX beam towards the measurement antenna. Continuously send uplink power control "up" commands in every uplink scheduling information to the UE; allow at least 200 ms for the UE to reach P_{UMAX}. Allow at least BEAM_SELECT_WAIT_TIME (defined in Annex K.1.1 of TS 38.521-2 [11]) for the UE RX beam selection to complete.
4. Determine EIS ($Pol_{Meas}=\theta$, $Pol_{Link}=\theta$) for θ-polarization, i.e., the power level for the θ-polarization, at which the throughput exceeds the requirements for the specified reference measurement channel. For power steps near the sensitivity level, measure the average throughput for a duration sufficient to achieve statistical significance according to Annex H.2.2 of TS 38.521-2 [11]. The downlink power step size shall be no more than 0.2 dB when the RF power level is near the sensitivity level.
5. Connect the SS (System Simulator) with the DUT through the measurement antenna with $Pol_{Link}=\phi$ polarization to form the RX beam towards the measurement antenna. Continuously send uplink power control "up" commands in every uplink scheduling

information to the UE; allow at least 200 ms for the UE to reach P_{UMAX}. Allow at least BEAM_SELECT_WAIT_TIME for the UE RX beam selection to complete.

6. Determine EIS ($Pol_{Meas}=\phi$, $Pol_{Link}=\phi$) for ϕ-polarization, i.e., the power level for the ϕ-polarization, at which the throughput exceeds the requirements for the specified reference measurement channel. For power steps near the sensitivity level, measure the average throughput for a duration sufficient to achieve statistical significance according to Annex H.2.2 of TS 38.521-2 [11]. The downlink power step size shall be no more than 0.2 dB when the RF power level is near the sensitivity level.
7. Advance to the next grid point and repeat steps 3 through 6 until measurements within the zenith range of $0^o \leq \theta \leq 90^o$ have been completed
8. After the measurements within zenith range $0^o \leq \theta \leq 90^o$ have been completed and
    a. If the re-positioning concept is applied to the RX test cases, position the device in DUT Orientation 2 (either Options 1 or 2) from Table A.1-1 through Table A.1-3 for the Alignment Option selected in Step 1. For the RX beam peak search in the second hemisphere, perform steps 3 through 6 for the range of zenith angles $90^o < \theta \leq 0^o$.
    b. If the re-positioning concept is not applied to the RX test cases, continue steps 3 through 6 for the range of zenith angles $90^o < \theta \leq 180^o$
9. Calculate the resulting averaged EIS for each grid point as:

$$EIS_{avg} = 2*[1/EIS\ (Pol_{Meas}=\theta,\ Pol_{Link}=\theta) + 1/EIS\ (Pol_{Meas}=\phi,\ Pol_{Link}=\phi)]^{-1}$$

The RX beam peak direction is where the minimum EIS_{avg} is found.

6.2 REFSENS – EIS

The intent of this test procedure is to measure the averaged EIS in the RX beam peak direction found in Section 6.1.

The EN-DC connections are established as outlined in Section 6.1. The test conditions defined in Table 6.1-1 apply for this test case.

The test procedure for is defined as follows:

1. Select any of the three Alignment Options (1, 2, or 3) from Table A.1-1 through Table A.1-3 to mount the DUT inside the QZ.
2. If the re-positioning concept is not applied to the RX test cases, position the device in DUT Orientation 1. If the re-positioning concept is applied to the RX test cases:
    a. position the device in DUT Orientation 1 from Table A.1-1 through Table A.1-3 if the maximum beam peak direction is within zenith angular range $0^o \leq \theta \leq 90^o$ for the alignment option selected in step 1,
    b. position the device in DUT Orientation 2 (either Options 1 or 2) from Table A.1-1 through Table A.1-3 if the maximum beam peak direction is within zenith angular range $90^o < \theta \leq 180^o$ for DUT Orientation 1 for the alignment option selected in step 1.
3. Connect the SS (System Simulator) with the DUT through the measurement antenna with $Pol_{Link}=\theta$ polarization to form the RX beam towards the RX beam peak direction. Continuously send uplink power control "up" commands in every uplink scheduling information to the UE; allow at least 200 ms for the UE to reach P_{UMAX}. Allow at least

BEAM_SELECT_WAIT_TIME (defined in Annex K.1.1 of TS 38.521-2 [11] for the UE RX beam selection to complete.

4. Determine EIS ($Pol_{Meas}=\theta$, $Pol_{Link}=\theta$) for θ-polarization, i.e., the power level for the θ-polarization at which the throughput exceeds the requirements for the specified reference measurement channel. For power steps near the sensitivity level, measure the average throughput for a duration sufficient to achieve statistical significance according to Annex H.2.2 of TS 38.521-2 [11]. The downlink power step size shall be no more than 0.2 dB when the RF power level is near the sensitivity level.
5. Connect the SS (System Simulator) with the DUT through the measurement antenna with $Pol_{Link}=\phi$ polarization to form the RX beam towards the RX beam peak direction. Continuously send uplink power control "up" commands in every uplink scheduling information to the UE; allow at least 200 ms for the UE to reach P_{UMAX}. Allow at least BEAM_SELECT_WAIT_TIME for the UE RX beam selection to complete.
6. Determine EIS($Pol_{Meas}=\phi$, $Pol_{Link}=\phi$) for ϕ-polarization, i.e., the power level for the ϕ-polarization at which the throughput exceeds the requirements for the specified reference measurement channel. For power steps near the sensitivity level, measure the average throughput for a duration sufficient to achieve statistical significance according to Annex H.2.2 of TS 38.521-2 [11] The downlink power step size shall be no more than 0.2 dB when the RF power level is near the sensitivity level.
7. Calculate the resulting averaged EIS in the RX beam peak direction as:

   $EIS_{avg} = 2*[1/EIS\ (Pol_{Meas}=\theta, Pol_{Link}=\theta) + 1/EIS\ (Pol_{Meas}=\phi, Pol_{Link}=\phi)]^{-1}$

6.3 REFSENS – Spherical Coverage

The intent of this test procedure is to verify that the spatial coverage of the UE in the expected directions is acceptable.

The test conditions defined in Table 6.1-1 apply for this test case.

The $EIS_{50\%\text{-}CCDF}$ is obtained from the Complementary Cumulative Distribution Function (CCDF) computed from the EIS_{avg} measurements for all grid points collected during the RX beam peak search in Section 6.1. Alternatively, the $EIS_{50\%\text{-}CCDF}$ can be obtained from the CCDF computed from the EIS_{avg} measurements using the procedure outlined in Section 6.1 but for the minimum number of grid points outlined in Appendix D.4.

When using constant step size measurement grids, a theta-dependent correction shall be applied, i.e., the PDF probability contribution for each measurement point is scaled by the normalized Clenshaw-Curtis weights $W(\theta)/W(\theta=90^{o})$ as outlined in Appendix D.2.

Section 7 Measurement Uncertainty

7.1 EIRP Tests

The Effective Isotropic Radiated Power (EIRP) test method determines the unknown performance of the DUT by correcting the absolute power measurements at the input port of the test instrumentation using a relative correction value determined using the range reference measurement described in Section 4 correction value offsets each power measurement back to the equivalent power that would have been radiated by a theoretical isotropic radiator in order to produce the same measured level. This corrected value is known as the Effective Isotropic Radiated Power.

In Table 7.1-1, uncertainties are identified that belong to either the DUT measurement, the Range Reference Measurement Stage or both for the EIRP test case.

Table 7.1-1 Uncertainty Contributions for EIRP Measurements

UID	Description Of Uncertainty Contributions	Reference
Stage 2: DUT Measurement		
1	Positioning Misalignment	See Appendix C.2
2	Measurement Distance	See Appendix C.3
3	Quality of Quiet Zone	See Appendix C.4
4	Mismatch	See Appendix C.5
5	Chamber Standing Wave	See Appendix C.6
6	RF Power Measurement Equipment	See Appendix C.7
7	Phase Curvature	See Appendix C.9
8	Amplifiers	See Appendix C.10
9	Random Uncertainty	See Appendix C.11
10	Influence of the XPD	See Appendix C.12
11	Multiple Measurement Antennas	See Appendix C.14
12	DUT Repositioning	See Appendix C.15
Stage 1: Range Reference Measurement		
13	Mismatch	See Appendix C.5
14	Amplifiers	See Appendix C.10
15	Misalignment of Positioning System	See Appendix C.17
16	Network Analyzer	See Appendix C.18
17	Absolute Gain of the Calibration Antenna	See Appendix C.19
18	Positioning and Pointing Misalignment between the Reference Antenna and the Measurement Antenna	See Appendix C.20
19	Phase Center Offset of Calibration Antenna	See Appendix C.21
20	Quality of Quiet Zone for Calibration Process	See Appendix C.22
21	Influence of the Calibration Antenna Feed Path	See Appendix C.23
22	Standing Wave between Reference Calibration Antenna and Measurement Antenna	See Appendix C.24
23	Insertion Loss Variation	See Appendix C.25
Systematic Uncertainties		
24	Influence of Noise	See Appendix C.26
25	Systematic Error related to Beam Peak Search	See Appendix C.27

7.2 TRP Tests

The Total Radiated Power (TRP) test method is based on the EIRP approach outlined in Section 7.1 but requires the integration of EIRPs across the total spherical surface to determine the Total Radiated Power.

In Table 7.2-1, uncertainties are identified that belong to either the DUT measurement, the Range Reference Measurement Stage or both for the TRP test case.

Table 7.2-1 Uncertainty Contributions for TRP Measurements

UID	Description of Uncertainty Contributions	Reference
Stage 2: DUT Measurement		
1	Positioning Misalignment	See Appendix C.2
2	Measurement Distance	See Appendix C.3
3	Quality of Quiet Zone	See Appendix C.4
4	Mismatch	See Appendix C.5
5	Chamber Standing Wave	See Appendix C.6
6	RF Power Measurement Equipment	See Appendix C.7
7	Phase Curvature	See Appendix C.9
8	Amplifiers	See Appendix C.10
9	Random Uncertainty	See Appendix C.11
10	Influence of the XPD	See Appendix C.12
11	Influence of TRP Measurement Grid	See Appendix C.13
12	Multiple Measurement Antennas	See Appendix C.14
13	DUT Repositioning	See Appendix C.15
Stage 1: Range Reference Measurement		
14	Mismatch	See Appendix C.5
15	Amplifiers	See Appendix C.10
16	Misalignment of Positioning System	See Appendix C.17
17	Network Analyzer	See Appendix C.18
18	Absolute Gain of the Calibration Antenna	See Appendix C.19
19	Positioning and Pointing Misalignment between the Reference Antenna and the Measurement Antenna	See Appendix C.20
20	Phase Center Offset of Calibration Antenna	See Appendix C.21
21	Quality of Quiet Zone for Calibration Process	See Appendix C.22
22	Influence of the Calibration Antenna Feed Path	See Appendix C.23
23	Standing Wave between Reference Calibration Antenna and Measurement Antenna	See Appendix C.24
24	Insertion Loss Variation	See Appendix C.25
Systematic Uncertainties		
25	Influence of Noise	See Appendix C.26

7.3 EIRP Spherical Coverage

The EIRP Spherical Coverage test method is based on the EIRP approach outlined in Section 7.1 but requires the computation of the Cumulative Distribution Function (CDF) of EIRPs measured on each grid point of the spherical surface.

In Table 7.3-1, uncertainties are identified that belong to either the DUT measurement, the Range Reference Measurement Stage or both for the EIRP spherical coverage test case.

Table 7.3-1 Uncertainty Contributions for EIRP Spherical Coverage Measurements

UID	Description of Uncertainty Contributions	Reference
Stage 2: DUT Measurement		
1	Positioning Misalignment	See Appendix C.2
2	Measurement Distance	See Appendix C.3
3	Quality of Quiet Zone	See Appendix C.4
4	Mismatch	See Appendix C.5
5	Chamber Standing Wave	See Appendix C.6
6	RF Power Measurement Equipment	See Appendix C.7
7	Phase Curvature	See Appendix C.9
8	Amplifiers	See Appendix C.10
9	Random Uncertainty	See Appendix C.11
10	Influence of the XPD	See Appendix C.12
11	Multiple Measurement Antennas	See Appendix C.14
12	DUT Repositioning	See Appendix C.15
13	Influence of Spherical Coverage Grid	See Appendix C.16
Stage 1: Range Reference Measurement		
14	Mismatch	See Appendix C.5
15	Amplifiers	See Appendix C.10
16	Misalignment of Positioning System	See Appendix C.17
17	Network Analyzer	See Appendix C.18
18	Absolute Gain of the Calibration Antenna	See Appendix C.19
19	Positioning and Pointing Misalignment between the Reference Antenna and the Measurement Antenna	See Appendix C.20
20	Phase Center Offset of Calibration Antenna	See Appendix C.21
21	Quality of Quiet Zone for Calibration Process	See Appendix C.22
22	Influence of the Calibration Antenna Feed Path	See Appendix C.23
23	Standing Wave between Reference Calibration Antenna and Measurement Antenna	See Appendix C.24
24	Insertion Loss Variation	See Appendix C.25
Systematic Uncertainties		
25	Influence of Noise	See Appendix C.26

7.4 EIS Tests

The Effective Isotropic Sensitivity (EIS) test method is similar to the EIRP method above, in that the range reference measurement is used to correct the unknown performance of the DUT back to values relative to that of a theoretical isotropic receiver. In this case, the correction value offsets each sensitivity level measurement back to the equivalent sensitivity level of a theoretical isotropic receiver exposed to an incoming isotropic wave with the same magnitude. This corrected value is known as the Effective Isotropic Sensitivity.

In Table 7.4-1, uncertainties are identified that belong to either the DUT measurement, the Range Reference Measurement Stage or both for the EIS test case.

Table 7.4-1 Uncertainty Contributions for EIS Measurements

UID	Description of Uncertainty Contributions	Reference
Stage 2: DUT Measurement		
1	Positioning Misalignment	See Appendix C.2
2	Measurement Distance	See Appendix C.3
3	Quality of Quiet Zone	See Appendix C.4
4	Mismatch	See Appendix C.5
5	Chamber Standing Wave	See Appendix C.6
6	gNB Emulator	See Appendix C.8
7	Phase Curvature	See Appendix C.9
8	Amplifiers	See Appendix C.10
9	Random Uncertainty	See Appendix C.11
10	Influence of the XPD	See Appendix C.12
11	Multiple Measurement Antennas	See Appendix C.14
12	DUT Repositioning	See Appendix C.15
Stage 1: Range Reference Measurement		
13	Mismatch	See Appendix C.5
14	Amplifiers	See Appendix C.10
15	Misalignment of Positioning System	See Appendix C.17
16	Network Analyzer	See Appendix C.18
17	Absolute Gain of the Calibration Antenna	See Appendix C.19
18	Positioning and Pointing Misalignment between the Reference Antenna and the Measurement Antenna	See Appendix C.20
19	Phase Center Offset of Calibration Antenna	See Appendix C.21
20	Quality of Quiet Zone for Calibration Process	See Appendix C.22
21	Influence of the Calibration Antenna Feed Path	See Appendix C.23
22	Standing Wave between Reference Calibration Antenna and Measurement Antenna	See Appendix C.24
23	Insertion Loss Variation	See Appendix C.25
Systematic Uncertainties		
24	Systematic Error related to Beam Peak Search	See Appendix C.27

7.5 EIS Spherical Coverage

The EIS Spherical Coverage test method is based on the EIS approach outlined in Section 7.4 but requires the computation of the Complementary Cumulative Distribution Function (CCDF) of EISs measured on each grid point of the spherical surface.

In Table 7.5-1, uncertainties are identified that belong to either the DUT measurement, the Range Reference Measurement Stage or both for the EIS spherical coverage test case.

Table 7.5-1 Uncertainty Contributions for EIS Spherical Coverage Measurements

UID	Description of Uncertainty Contributions	Reference
Stage 2: DUT Measurement		
1	Positioning Misalignment	See Appendix C.2
2	Measurement Distance	See Appendix C.3
3	Quality of Quiet Zone	See Appendix C.4
4	Mismatch	See Appendix C.5
5	Chamber Standing Wave	See Appendix C.6
6	gNB Emulator	See Appendix C.8
7	Phase Curvature	See Appendix C.9
8	Amplifiers	See Appendix C.10
9	Random Uncertainty	See Appendix C.11
10	Influence of the XPD	See Appendix C.12
11	Multiple Measurement Antennas	See Appendix C.14
12	DUT Repositioning	See Appendix C.15
13	Influence of Spherical Coverage Grid	See Appendix C.16
Stage 1: Range Reference Measurement		
14	Mismatch	See Appendix C.5
15	Amplifiers	See Appendix C.10
16	Misalignment of Positioning System	See Appendix C.17
17	Network Analyzer	See Appendix C.18
18	Absolute Gain of the Calibration Antenna	See Appendix C.19
19	Positioning and Pointing Misalignment between the Reference Antenna and the Measurement Antenna	See Appendix C.20
20	Phase Center Offset of Calibration Antenna	See Appendix C.21
21	Quality of Quiet Zone for Calibration Process	See Appendix C.22
22	Influence of the Calibration Antenna Feed Path	See Appendix C.23
23	Standing Wave between Reference Calibration Antenna and Measurement Antenna	See Appendix C.24
24	Insertion Loss Variation	See Appendix C.25
Systematic Uncertainties		
25	Systematic error related to EIS spherical coverage	See Appendix C.26

7.6 Calculation of the Total Expanded Measurement Uncertainty

The ISO guide [1] gives a general approach to calculating measurement uncertainty that is applicable to all types of measurements; the process involving the combination of the standard deviations (known as standard uncertainties) of the individual contributors by the root-sum of squares method. This method assumes that all systematic errors have been identified and corrected, and that any remaining errors in individual uncertainty components are random in nature such that they can be combined as normal distributions. Note that this may not be the case when combining multiple identical measurements in series. Likewise, multiple parallel measurements (e.g., the different paths in the test system) do not reduce the systematic error contribution through averaging.

Using the above approach to determine the method for uncertainty analysis, the following illustrates the practical steps involved:

1. Compile a complete list of the individual measurement uncertainties that contribute to a measurement.
2. Determine the maximum value of each uncertainty.
3. Determine the distribution of each uncertainty (rectangular, U-shaped, etc.)

4. Calculate (if necessary) the standard deviation of each uncertainty, u_i, for each uncertainty.

5. Convert the units (if necessary) of each uncertainty into the chosen unit, i.e., dB.

6. Combine ALL the standard uncertainties by the root-sum-squares method to derive the 'combined standard uncertainty'.

7. Under the assumption that the probability distribution of the combined standard uncertainty is Gaussian/Normal, multiply the resulting combined standard uncertainty by an expansion factor 'k' (taken from Student's T-distribution, W.S. Gosset 1908) to derive the 'expanded uncertainty' for a given confidence level. All expanded uncertainties are quoted to 95% confidence level, so k is taken as 2 (theoretically k should be 1.96, but for convenience, the value 2 had been agreed). Expressed a different way, this gives 95% confidence that the true value is within 2 times the combined standard uncertainty of the measured value to derive the ‘expanded uncertainty’.

8. Any systematic errors that cannot be eliminated are added to the expanded uncertainty to derive the ‘total expanded uncertainty’, i.e.:

$$u_{c,\text{total expanded}} = u_{c,\text{expanded}} + u_{c,\text{systematic}} = 1.96\sqrt{\sum u_i^2} + \sum u_{i,\text{systematic}}$$

It is not suggested that this process be carried out at every individual test frequency since this would be extremely time consuming and tedious. Rather, the measurement uncertainty evaluation shall be carried out for each of the FR2 sub ranges defined in Table 3.3-1, i.e., all the uncertainties should be evaluated over the entire frequency range for that band and the worst-case values within the band taken and used in the calculations. Admittedly, this could lead to slightly pessimistic overall values, but the bonus is in reduced measurement time and a one-hit process that will be applicable to any frequency within the relevant band.

7.7 Criteria – Maximum Test System Uncertainty

The results of the calculations for expanded uncertainty for all test cases measurements shall be reported, along with full documentation to support the resulting values. The test performance requirements shall not be adjusted by the measurement uncertainty when determining compliance of the DUTs.

The expanded uncertainties must not exceed the maximum test system uncertainty values in Table 7.7-1 at a 95% confidence level.

Table 7.7-1 Maximum Test System Uncertainty for Different Test Cases

Expanded Uncertainty [dB]				
Test Case	**FR2_1 (24.25GHz- 32GHz)**	**FR2_2 (32 GHz - 40 GHz)**	**FR2_3 (40 GHz - 48 GHz)**	**FR2_4 (48 GHz - 52.6GHz)**
Maximum Output Power – EIRP	4.79	4.99	TBD	TBD
Maximum Output Power – TRP	4.31	4.51	TBD	TBD
Maximum Output Power – Spherical Coverage	4.49	5.09	TBD	TBD
REFSENS – EIS	5.10	5.10	TBD	TBD
REFSENS – Spherical Coverage	4.80	4.80	TBD	TBD

Appendix A Test Setup Configurations

A.1 Positioning Requirements and Reference Coordinate System

This appendix defines the measurement coordinate system for the NR UE. The reference coordinate system is provided in Figure A.1-1 for the DUT in the default alignment, i.e., the DUT and the fixed system coordinate systems are aligned with $\Psi = 0^o$ and $\Theta = 0^o$ and $\Phi = 0^o$ where Ψ, Θ, and Φ describe the relative angles between the two coordinate systems.

Figure A.1-1 Reference Coordinate System

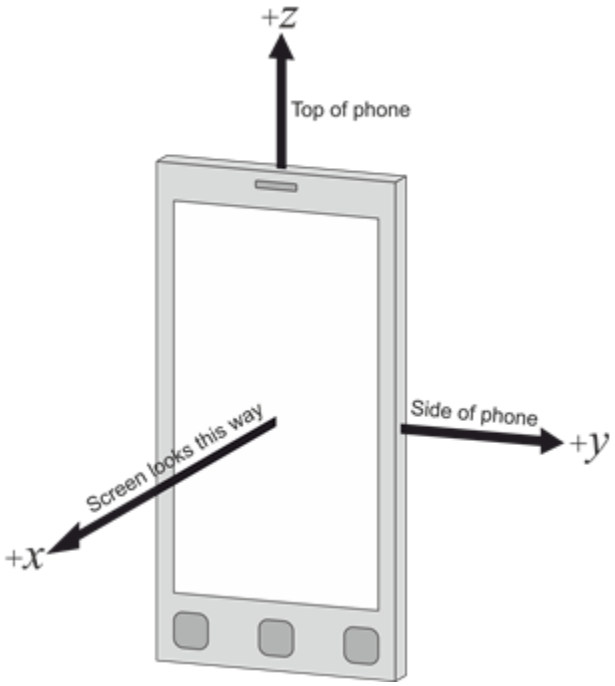

The following aspects are necessary:

- A basic understanding of the top and bottom of the device is needed in order to define unambiguous DUT positioning requirements for the test, e.g., in the drawings used in this appendix, the three buttons are on the bottom of the device (front) and the camera is on the top of the device (back)
- An understanding of the origin and alignment of the coordinate system inside the test system, i.e. the directions in which the x, y, z axes point inside the test chamber, in order to define unambiguous DUT orientation, DUT beam, signal, interference, and measurement angles

The tables below provide the test conditions and angle definitions for three permitted device alignments for the default test condition, DUT orientation 1, and two different options for each permitted device alignment to re-position the device for DUT Orientation 2 as outlined in Figure A.1-2 and Figure A.1-3.

Table A.1-1 Test Conditions and Angle Definitions for Alignment Option 1

Test condition	DUT orientation	Link angle	Measurement angle	Diagram
Free space DUT Orientation 1 (default)	$\Psi = 0^o$ $\Theta = 0^o$ $\Phi = 0^o$	θ_{Link}; ϕ_{Link} with polarization reference $Pol_{Link} = \theta$ or ϕ	θ_{Meas}; ϕ_{Meas} with polarization reference $Pol_{Meas} = \theta$ or ϕ	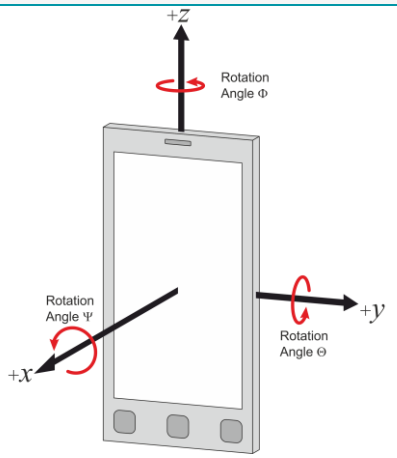
Free space DUT Orientation 2 - Option 1 (based on re-positioning approach)	$\Psi = 180^o$ $\Theta = 0^o$ $\Phi = 0^o$	θ_{Link}; ϕ_{Link} with polarization reference $Pol_{Link} = \theta$ or ϕ	θ_{Meas}; ϕ_{Meas} with polarization reference $Pol_{Meas} = \theta$ or ϕ	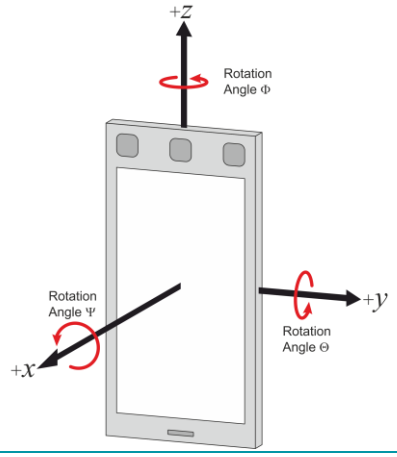
Free space DUT Orientation 2 - Option 2 (based on re-positioning approach)	$\Psi = 0^o$ $\Theta = 180^o$ $\Phi = 0^o$	θ_{Link}; ϕ_{Link} with polarization reference $Pol_{Link} = \theta$ or ϕ	θ_{Meas}; ϕ_{Meas} with polarization reference $Pol_{Meas} = \theta$ or ϕ	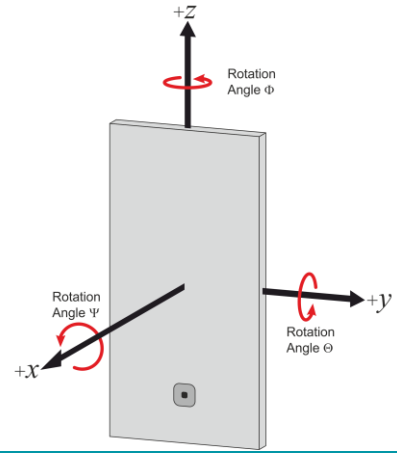

Note 1: A polarization reference, as defined in relation to the reference coordinate system, is maintained for each link and measurement angle
Note 2: The order of rotation angles listed in the DUT orientation column corresponds to the necessary order of rotations.

Table A.1-2 Test Conditions and Angle Definitions for Alignment Option 2

Test condition	DUT orientation	Link angle	Measurement angle	Diagram
Free space DUT Orientation 1 (default)	$\Psi = 0^o$ $\Theta = -90^o$ $\Phi = 0^o$	θ_{Link}; ϕ_{Link} with polarization reference $Pol_{Link} = \theta$ or ϕ	θ_{Meas}; ϕ_{Meas} with polarization reference $Pol_{Meas} = \theta$ or ϕ	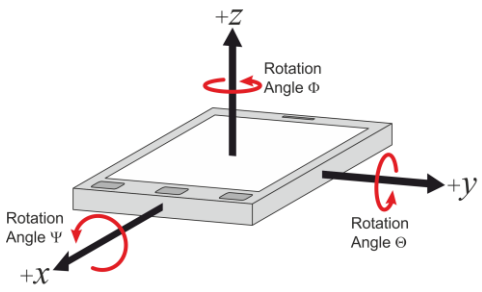
Free space DUT Orientation 2 - Option 1 (based on re-positioning approach)	$\Psi = 180^o$ $\Theta = 90^o$ $\Phi = 0^o$	θ_{Link}; ϕ_{Link} with polarization reference $Pol_{Link} = \theta$ or ϕ	θ_{Meas}; ϕ_{Meas} with polarization reference $Pol_{Meas} = \theta$ or ϕ	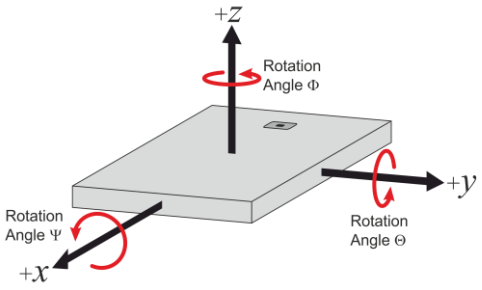
Free space DUT Orientation 2 - Option 2 (based on re-positioning approach)	$\Psi = 0^o$ $\Theta = 90^o$ $\Phi = 0^o$	θ_{Link}; ϕ_{Link} with polarization reference $Pol_{Link} = \theta$ or ϕ	θ_{Meas}; ϕ_{Meas} with polarization reference $Pol_{Meas} = \theta$ or ϕ	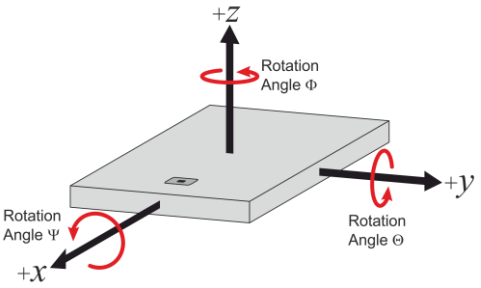

Note 1: A polarization reference, as defined in relation to the reference coordinate system, is maintained for each link and measurement angle
Note 2: The order of rotation angles listed in the DUT orientation column corresponds to the necessary order of rotations.

Table A.1-3 Test Conditions and Angle Definitions for Alignment Option 3

Test condition	DUT orientation	Link angle	Measurement angle	Diagram
Free space DUT Orientation 1 (default)	$\Psi = 90^o$ $\Theta = 0^o$ $\Phi = 0^o$	θ_{Link}; ϕ_{Link} with polarization reference $Pol_{Link} = \theta$ or ϕ	θ_{Meas}; ϕ_{Meas} with polarization reference $Pol_{Meas} = \theta$ or ϕ	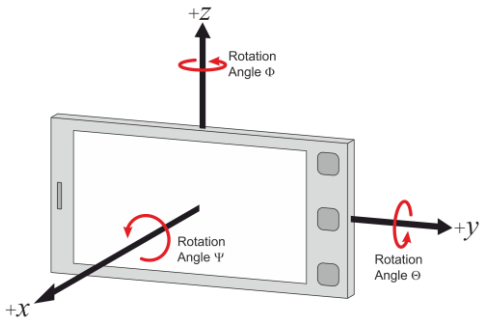
Free space DUT Orientation 2 - Option 1 (based on re-positioning approach)	$\Psi = -90^o$ $\Theta = 0^o$ $\Phi = 0^o$	θ_{Link}; ϕ_{Link} with polarization reference $Pol_{Link} = \theta$ or ϕ	θ_{Meas}; ϕ_{Meas} with polarization reference $Pol_{Meas} = \theta$ or ϕ	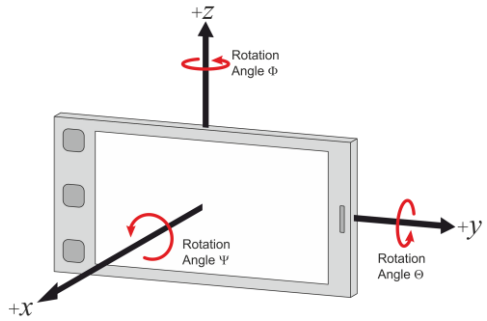
Free space DUT Orientation 2 - Option 2 (based on re-positioning approach)	$\Psi = 90^o$ $\Theta = 180^o$ $\Phi = 0^o$	θ_{Link}; ϕ_{Link} with polarization reference $Pol_{Link} = \theta$ or ϕ	θ_{Meas}; ϕ_{Meas} with polarization reference $Pol_{Meas} = \theta$ or ϕ	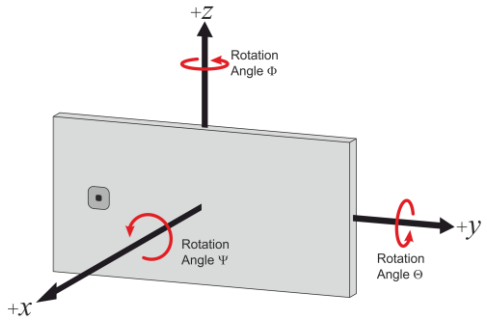
Note 1: A polarization reference, as defined in relation to the reference coordinate system, is maintained for each link and measurement angle Note 2: The order of rotation angles listed in the DUT orientation column corresponds to the necessary order of rotations.				

For each UE requirement and test case, each of the parameters in the tables above need to be recorded, such that DUT positioning, DUT beam direction, and angles link and measurement are specified in terms of the fixed system coordinate system.

Due to the non-commutative nature of rotations, the order of rotations is important and needs to be defined when multiple DUT orientations are tested.

The following order of rotations needs to be followed for the device orientations specified in this test plan: Ψ (rotation around the x axis) → Θ (rotation around the y axis) → Φ (rotation around the z axis).

The rotations around the x, y, and z axes can be defined with the following rotation matrices:

$$R_x(\Psi) = \begin{bmatrix} 1 & 0 & 0 & 0 \\ 0 & \cos\Psi & -\sin\Psi & 0 \\ 0 & \sin\Psi & \cos\Psi & 0 \\ 0 & 0 & 0 & 1 \end{bmatrix}$$

$$R_y(\Theta) = \begin{bmatrix} \cos\Theta & 0 & \sin\Theta & 0 \\ 0 & 1 & 0 & 0 \\ -\sin\Theta & 0 & \cos\Theta & 0 \\ 0 & 0 & 0 & 1 \end{bmatrix}$$

and

$$R_z(\Phi) = \begin{bmatrix} \cos\Phi & -\sin\Phi & 0 & 0 \\ \sin\Phi & \cos\Phi & 0 & 0 \\ 0 & 0 & 1 & 0 \\ 0 & 0 & 0 & 1 \end{bmatrix}.$$

with the respective angles of rotation Ψ, Θ, and Φ and:

$$\begin{bmatrix} x' \\ y' \\ z' \\ 1 \end{bmatrix} = R \begin{bmatrix} x \\ y \\ z \\ 1 \end{bmatrix}$$

Additionally, any translation of the DUT can be defined with the translation matrix:

$$T(t_x, t_y, t_z) = \begin{bmatrix} 1 & 0 & 0 & t_x \\ 0 & 1 & 0 & t_y \\ 0 & 0 & 1 & t_z \\ 0 & 0 & 0 & 1 \end{bmatrix}$$

with offsets t_x, t_y, t_z in x, y, and z, respectively and with:

$$\begin{bmatrix} x' \\ y' \\ z' \\ 1 \end{bmatrix} = T \begin{bmatrix} x \\ y \\ z \\ 1 \end{bmatrix}$$

The combination of rotations and translation is captured by the multiplication of rotation and translation matrices.

For this test plan, the matrix M is defined as:

$$M = R_z(\Phi) \cdot R_y(\Theta) \cdot R_x(\Psi)$$

which describes an initial rotation of the DUT around the x axis with angle Ψ, a subsequent rotation around the y axis with angle Θ, and a final rotation around the z axis with angle Φ.

The DUT coordinates can then be determined from the measurement/chamber coordinates using the following equation:

$$r_{\mathrm{EUT}} = \begin{bmatrix} x_{\mathrm{EUT}} \\ y_{\mathrm{EUT}} \\ z_{\mathrm{EUT}} \end{bmatrix} = M^{-1} \cdot r_{\mathrm{DUT}} = M^{-1} \cdot \begin{bmatrix} x_{\mathrm{Meas}} \\ y_{\mathrm{Meas}} \\ z_{\mathrm{Meas}} \end{bmatrix} = M^{-1} \cdot \begin{bmatrix} \sin(\theta_{Meas})\cos(\phi_{Meas}) \\ \sin(\theta_{Meas})\sin(\phi_{Meas}) \\ \cos(\theta_{Meas}) \end{bmatrix}$$

with

$$\theta_{\mathrm{EUT}} = \mathrm{acos}(z_{\mathrm{EUT}})$$ and

$$\phi_{\mathrm{EUT}} = \mathrm{atan}(y_{\mathrm{EUT}} / x_{\mathrm{EUT}})$$

The center of the reference coordinate system shall be aligned with the geometric center of the DUT in order to minimize the offset between antenna arrays integrated at any position of the UE and the center of the quiet zone.

Near-field coupling effects between the antenna and the pedestals/positioners/fixtures generally cause increased signal ripples. Re-positioning the DUT in order to direct the beam peak away from those areas can reduce the effect of signal ripple on EIRP/EIS measurements. The figures below illustrate how the DUT is repositioned within the distributed axes and combined axes system, when:

- The beam peak is directed to the DUTs upper hemisphere (DUT orientation 1) or
- The beam peak is directed to the DUTs lower hemisphere (DUT orientation 2).

While these figures are examples of different positioning systems and other implementations are not precluded, the relative orientation of the coordinate system with respect to the antennas/reflectors and the axes of rotation shall apply to any measurement setup.

Figure A.1-2 DUT Re-Positioning for an Example of Distributed-Axes System

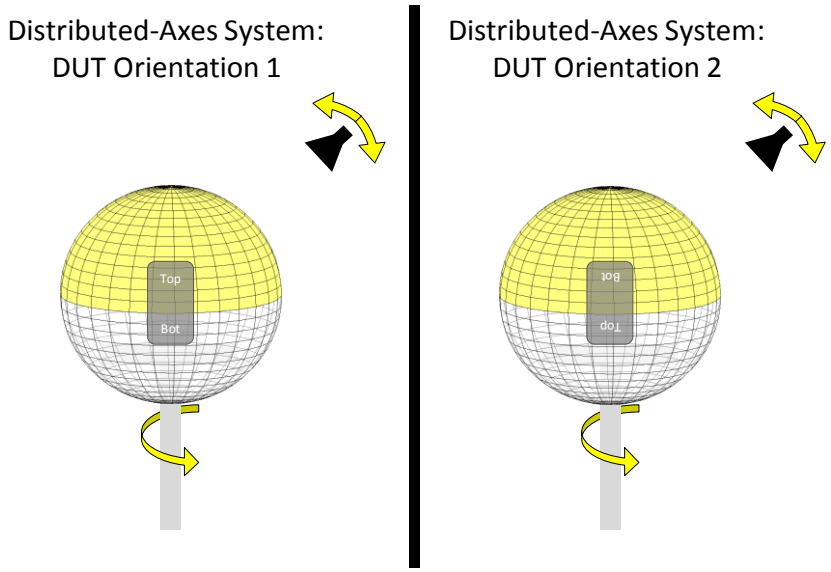

Figure A.1-3 DUT Re-Positioning for an Example of Combined-Axes System

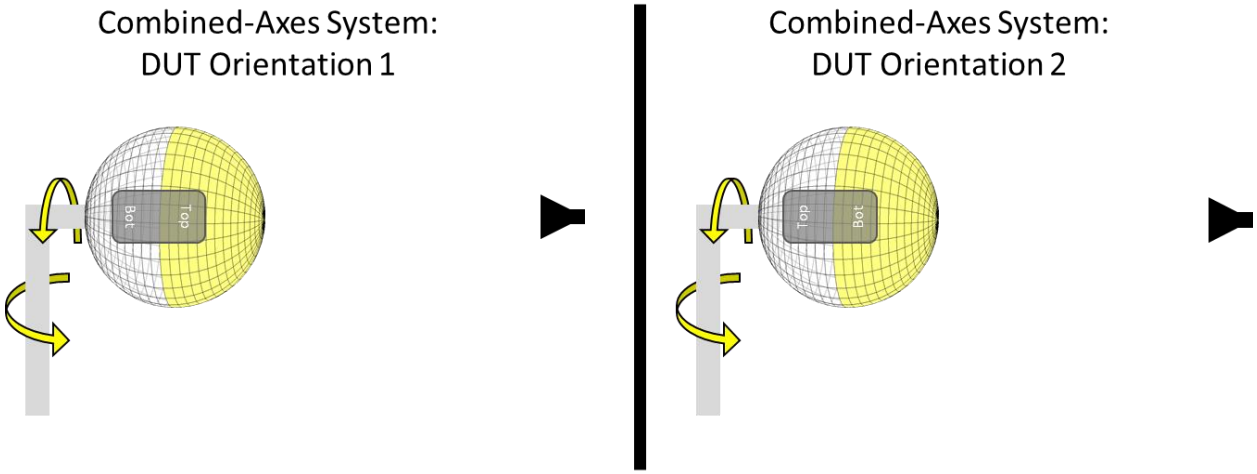

For EIRP/EIS measurements, it is important to re-position the DUT to ensure the pedestal is not obstructing the beam path and to ensure that the pedestal is not in closer proximity to the measurement antenna/reflector than the DUT. For TRP measurements, re-positioning the DUT ensures that the beam peak direction is not obstructed by the pedestal and the pedestal is in the measurement path only when measuring the DUT' back-hemisphere. No re-positioning if the DUT during a TRP measurement is required.

A.2 Test Systems Setups

This section will be added at a later date.

A.3 Test Setup - Instrumentation

This section will be added at a later date.

Appendix B Phantom Definitions

This section is left blank. Phantoms will be added in a future version of the test plan.

Appendix C Measurement Uncertainty

C.1 Introduction

For the Millimeter-Wave Wireless Device Over-the-Air Performance described in this Test Plan, the chosen method for calculation of the measurement uncertainty is based on the “Guide to the Expression of Uncertainty in Measurement” [1].

The following subsections list all MU elements that are identified to have relevance for the measurement uncertainty budget in 5G Millimeter-Wave transmitter and receiver performance and associated uncertainty analysis using the IFF (CATR) test environment.

C.2 Positioning Misalignment

This contribution originates from the misalignment of the test direction and the beam peak direction of the measurement antenna due to imperfect rotation operation. The pointing misalignment may happen in both azimuth and elevation directions and the effect of the misalignment depends highly on the beam width of the beam under test. The same level of misalignment results in a larger measurement error for a narrower beam.

C.3 Measurement Distance

The cause of this uncertainty contributor is due to the reduction of distance between the measurement antenna and the DUT.

C.4 Quality of Quiet Zone

The Quality of the Quiet Zone procedure characterizes the quiet zone performance of the anechoic chamber, specifically the effect of reflections within the anechoic chamber including any positioners and support structures. The MU term additionally includes the amplitude variations effect of offsetting the directive antenna array inside a DUT from the center of the quiet zone as well as the directivity MU, i.e., the variation of antenna gains in the different direct line-of-sight links.

C.5 Mismatch

This uncertainty contribution addresses variation in the test system VSWR that introduces measurement uncertainty. For more information, see G.1 of [2]. The mismatch MU is reduced significantly by using a total system calibration, i.e., a combination of the cable calibration and range reference test, due to the elimination of common pairs. Special care must be taken for the environmental conditions (temperature, humidity, etc.) to remain stable over time to ensure that the phase and amplitude of the standing waves between the various system components remain the same between the system calibration and device measurements.

C.6 Chamber Standing Wave

This term accounts for a standing wave reflection between the measurement antenna and the DUT, representing an additional chamber ripple term beyond that recorded in the Quality of Quiet Zone validation. One method to obtain this value is to slide the DUT $\lambda/4$ towards the measurement antenna while measuring the amplitude. The uncertainty term can be derived by performing the standard deviation on the results. For more information, see G.7 of [2].

For the IFF methodology, the chamber standing wave assessment in G.7.3.2 of [2] is not applicable and the MU contribution is generally negligible.

C.7 RF Power Measurement Equipment

The receiving device is used to measure the received signal level in the EIRP measurements as an absolute level. For more information, see G.4 of [2].

C.8 gNB Emulator

gNB emulator is used to drive a signal to the measurement antenna (via multiple external components such as a switch box, an amplifier and a circulator, etc.) in sensitivity tests either as an absolute level or as a relative level. Generally, an uncertainty contribution from absolute level accuracy, non-linearity and frequency characteristic of the gNB emulator is introduced.

For more information, see G.5 of [2].

C.9 Phase Curvature

This contribution originates from the finite far field measurement distance, which causes phase curvature across the antenna of UE/reference antenna. At a measurement distance of $2D^2/\lambda$ the phase curvature is 22.5^o.

C.10 Amplifiers

For external amplifiers, the following uncertainties should be considered but the applicability is contingent to the measurement implementation and calibration procedure:

- Stability: an uncertainty contribution comes from the output level stability of the amplifier. Even if the amplifier is part of the system for both measurement and calibration, the uncertainty due to the stability shall be considered. This uncertainty can be either measured or determined by the manufacturers' data sheet for the operating conditions in which the system will be required to operate.

- Linearity: an uncertainty contribution comes from the linearity of the amplifier since in most cases calibration and measurements are performed at two different input/output power levels. This uncertainty can be either measured or determined by the manufacturers' data sheet.

- Noise Figure: when the signal goes into an amplifier, noise is added so that the SNR at the output is reduced with regards to the SNR of the signal at the input. This added noise introduces error on the signal which affects the Error Rate of the receiver thus the EVM (Error Vector Magnitude)

- Mismatch: if the external amplifier is used for both stages, measurement and calibration the uncertainty contribution associated with it can be considered systematic and constant -> 0 dB. If it is not the case, the mismatch uncertainty at its input and output shall be determined

- Gain: if the external amplifier is used for both stages, measurement and calibration the uncertainty contribution associated with it can be considered systematic and constant -> 0 dB. If it is not the case, this uncertainty shall be considered.

C.11 Random Uncertainty

This contribution is used to account for all the unknown, unquantifiable, etc. uncertainties associated with the measurements. Random uncertainty MU contributions are normally distributed.

The random uncertainty term, by definition, cannot be measured, or even isolated completely. However, past system definitions provide an empirical basis for a value. A value of 0.5 dB (when compared to

0.2 dB for <6 GHz OTA measurements) is suggested due to increased sensitivity to random effects in more complex, higher frequency NR test systems.

C.12 Influence of the XPD

This uncertainty is related to the measurement probe's polarization impurity, i.e., the propagation induced coupling of field components from the intended polarization into the un-intended cross-polarization and vice versa. The associated measurement uncertainty can be determined using the XPD (cross polarization discrimination) of the measurement probe.

A typical probe antenna can have XPD of 30 dB.

A transmission matrix and calibration setup as shown in Figure C.12.1 is considered here. Typically, a single-polarized reference antenna with known gain is placed at the center of the quiet zone and the total attenuation, L, between the reference antenna terminal and the feed antenna terminals is determined as part of the range reference calibration procedure.

Figure C.12.1 Calibration Setup

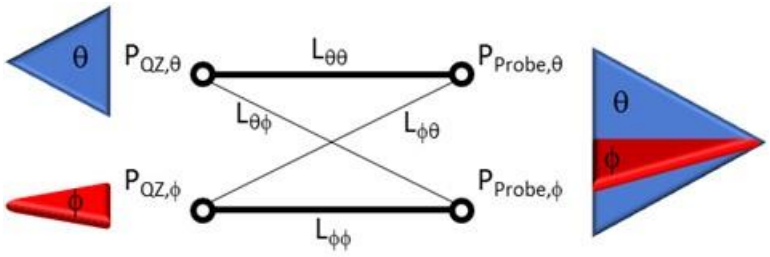

Since the reference antenna is considered a single-polarized antenna, the XPD effect is negligible. Since the measurement probe is assumed to be a dual-linearly polarized antenna, leakage from one terminal/polarization to the other, i.e., XPD, needs to be considered.

The dual-linearly polarized measurement probe has two terminals corresponding to a set of orthogonal polarizations, θ and ϕ which match the orientations of the reference antenna. The most thorough calibration procedure would determine the path losses between the four different combinations of signal paths: $\theta\theta$, $\theta\phi$, $\phi\theta$, and $\phi\phi$,, e.g., the power received by the measurement probe at the θ polarization/terminal, $P_{Feed,\theta}$, is attenuated by $L_{\phi\theta}$ with respect to the power delivered to the reference antenna oriented in the ϕ polarization and placed in the center of quiet zone, $P_{QZ,\phi}$.

The most common calibration approach, however, is based on calibrating the polarization matched paths in Figure C.12.1 (thick solid lines), i.e., $\theta\theta$ and $\phi\phi$. In this case, as illustrated in Figure C.12.2 the normalized pathlosses $L_{\theta\theta}$ and $L_{\phi\phi}$ are 1 and the pathlosses of the crossed components become the XPD terms of the measurement probe:

$$\alpha_{\theta\phi} = 10^{\frac{XPD_{\theta\phi}}{10}} \quad (1.1)$$

and

$$\alpha_{\phi\theta} = 10^{\frac{XPD_{\phi\theta}}{10}} \quad (1.2)$$

Figure C.12.2 Common Calibration Approach Based on Calibrating the Polarization Matched Signal Paths

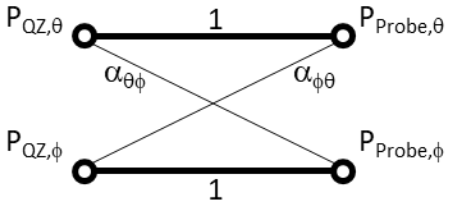

In the remainder of this analysis, it is assumed that the leakage between the two polarization ports of the measurement probe is assumed to be the same, i.e., XPD = $XPD_{\theta\phi}$ = $XPD_{\phi\theta}$ and $\alpha = \alpha_{\theta\phi} = \alpha_{\phi\theta}$.

The normalized powers at the measurement probe terminals can then be written as

$$P_{\text{Probe},\theta} = P_{\text{QZ},\theta} + \alpha P_{\text{QZ},\phi} \quad (1.3)$$

$$P_{\text{Probe},\phi} = P_{\text{QZ},\phi} + \alpha P_{\text{QZ},\theta} \quad (1.4)$$

The normalized ratio of total powers at measurement probe and the center of the quiet zone is therefore

$$\frac{\mathrm{P}_{\text{Probe}}}{\mathrm{P}_{\text{QZ}}} = \frac{\mathrm{P}_{\text{Probe},\theta} + \mathrm{P}_{\text{Probe},\phi}}{\mathrm{P}_{\text{QZ},\theta} + \mathrm{P}_{\text{QZ},\phi}} = \frac{\left(\mathrm{P}_{\text{QZ},\theta} + \mathrm{P}_{\text{QZ},\phi}\right)\left(1+\alpha\right)}{\mathrm{P}_{\text{QZ},\theta} + \mathrm{P}_{\text{QZ},\phi}} = 1+\alpha \quad (1.5)$$

This simple analysis shows that the XPD of the measurement system introduces a small error of the total power measured by the measurement probe and that the conservation of measured powers is not guaranteed, i.e., the MU based on the XPD can be expressed as

$$\mathrm{MU}_{XPD}\left[\mathrm{dB}\right] = 10\log_{10}\left(1+\alpha\right) = 10\log_{10}\left(1+10^{\frac{XPD}{10}}\right) \quad (1.6)$$

This XPD MU is tabulated for different levels of XPD in Table C.12 -1:

Table C.12 -1: XPD MU for Different XPD Values

XPD [dB]	MU_{XPD} [dB]
-20	0.043
-25	0.014
-30	0.004
-35	0.001
-40	0.000

When the range reference calibration is based on a full matrix-based approach, i.e., all signal paths are calibrated, the conservation of measured powers is guaranteed. As shown in Figure C.12.3, the polarization-matched signal paths take into account the leakage of power into the cross paths.

Figure C.12.3 Calibration Approach Based On Calibrating All Signal Paths

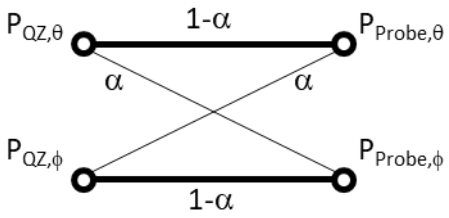

The powers at the measurement probe can now be written as

$$P_{\text{Probe},\theta} = (1-\alpha)P_{\text{QZ},\theta} + \alpha P_{\text{QZ},\phi} \quad (1.7)$$

$$P_{\text{Probe},\phi} = (1-\alpha)P_{\text{QZ},\phi} + \alpha P_{\text{QZ},\theta} \quad (1.8)$$

The normalized ratio of total powers at measurement probe and the center of the quiet zone is then

$$\frac{\mathrm{P}_{\text{Probe}}}{\mathrm{P}_{\text{QZ}}} = \frac{\mathrm{P}_{\text{Probe},\theta} + \mathrm{P}_{\text{Probe},\phi}}{\mathrm{P}_{\text{QZ},\theta} + \mathrm{P}_{\text{QZ},\phi}} = \frac{\mathrm{P}_{\text{QZ},\theta} + \mathrm{P}_{\text{QZ},\phi}}{\mathrm{P}_{\text{QZ},\theta} + \mathrm{P}_{\text{QZ},\phi}} = 1 \quad (1.9)$$

This simple analysis now shows that for a matrix-based calibration of all signal paths the XPD of the measurement probe no longer introduces any error and that the conservation of measured powers is guaranteed, i.e., the MU based on the XPD is 0 dB.

The derivation of the XPD MU based on powers is a more straightforward and less complex approach than with electric fields as attempted in [2]. This annex shows that the same XPU MU result as derived in (1.5) can be derived using electric fields.

The corresponding signal paths are illustrated in Figure C.12.4.

Figure C.12.4 Signal Paths For Electric Fields (Based On Calibrating The Polarization Matched Signal Paths)

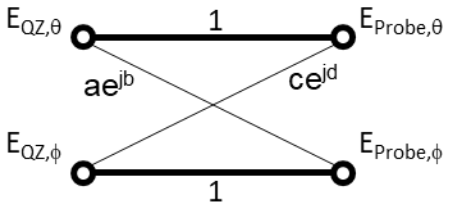

The normalized fields at the measurement probe terminals can then be written as

$$E_{\text{Probe},\theta} = E_{\text{QZ},\theta} + ce^{jd}E_{\text{QZ},\phi} \quad (1.10)$$

$$E_{\text{Probe},\phi} = E_{\text{QZ},\phi} + ae^{jb}E_{\text{QZ},\theta} \quad (1.11)$$

The transmission matrix can be defined as H

$$\begin{bmatrix} E_{\text{Probe},\theta} \\ E_{\text{Probe},\phi} \end{bmatrix} = H \begin{bmatrix} E_{\text{QZ},\theta} \\ E_{\text{QZ},\phi} \end{bmatrix} \quad (1.12)$$

with

$$H = \begin{bmatrix} 1 & ae^{jb} \\ ce^{jd} & 1 \end{bmatrix} \quad (1.13)$$

The total magnitude component of the electric field including coherence/interference terms at the probe is

$$\begin{aligned} E_{\text{Probe},T} &= \sqrt{\left|E_{\text{Probe},\theta}\right|^2 + \left|E_{\text{Probe},\phi}\right|^2} = \sqrt{\left|E_{\text{QZ},\theta} + ce^{jd}E_{\text{QZ},\phi}\right|^2 + \left|E_{\text{QZ},\phi} + ae^{jb}E_{\text{QZ},\theta}\right|^2} \\ &= \sqrt{\left[\left(E_{\text{QZ},\theta} + cE_{\text{QZ},\phi}\cos(d)\right)^2 + \left(cE_{\text{QZ},\phi}\sin(d)\right)^2\right] + \left[\left(E_{\text{QZ},\phi} + aE_{\text{QZ},\theta}\cos(b)\right)^2 + \left(aE_{\text{QZ},\theta}\sin(b)\right)^2\right]} \\ &= \sqrt{\begin{aligned}&\left[{E_{\text{QZ},\theta}}^2 + 2cE_{\text{QZ},\theta}E_{\text{QZ},\phi}\cos(d) + c^2{E_{\text{QZ},\phi}}^2\cos^2(d) + c^2{E_{\text{QZ},\phi}}^2\sin^2(d)\right] + \\ &\left[{E_{\text{QZ},\phi}}^2 + 2aE_{\text{QZ},\theta}E_{\text{QZ},\phi}\cos(b) + a^2{E_{\text{QZ},\theta}}^2\cos^2(b) + a^2{E_{\text{QZ},\theta}}^2\sin^2(b)\right]\end{aligned}} \\ &= \sqrt{{E_{\text{QZ},\theta}}^2\left(1+a^2\right) + {E_{\text{QZ},\phi}}^2\left(1+c^2\right) + 2E_{\text{QZ},\theta}E_{\text{QZ},\phi}\left(c\cos(d) + a\cos(b)\right)} \end{aligned} \quad (1.14)$$

When it is assumed that leakage between the two polarization ports of the measurement probe is assumed to be the same, then $a=c=10^{\text{XPD}/20}$ in (1.14). Additionally, it must be assumed that $d=b+\pi$ which guarantees the orthogonality between the two field vectors, i.e., the dot product between the vectors has to be zero. With these assumptions, Equation (1.14) will become

$$E_{\text{Probe},T} = \sqrt{\left(E_{\text{QZ},\theta}{}^2 + E_{\text{QZ},\phi}{}^2\right)\left(1+a^2\right)} \quad (1.15)$$

The normalized ratio of total powers at measurement probe and the center of the quiet zone is therefore

$$\frac{\text{P}_{\text{Probe}}}{\text{P}_{\text{QZ}}} \propto \frac{E_{\text{Probe},T}{}^2}{E_{\text{QZ},T}{}^2} = 1+a^2 = 1+10^{\frac{2\,XPD}{20}} = 1+10^{\frac{XPD}{10}} \quad (1.16)$$

The derived XPD MU based on electric fields which included the coherence/interference terms in (1.16) is the same as in (1.6).

The XPD of the measurement system shall be determined from the quality of quiet zone measurements, see Section 3.5 at the 7 reference points, P1 through P7, specifically with reference AUT orientations $\gamma=\beta=0^{\text{o}}$ for distributed axes systems, Section 3.5.1 or reference AUT orientations $\beta=\alpha=0^{\text{o}}$ for combined-axes systems, Section 3.5.2. Alternatively, it can be determined using a reference antenna optimized for XPD measurements and with the corresponding alignment to achieve optimal polarization matching between the reference and the measurement antenna.

The XPD for each reference point shall be calculated as the ratio of cross-polarized to co-polarized measured powers and the largest XPD from the 7 different reference points shall be used to determine the XPD MU, i.e.,

$$\text{MU}_{XPD}\left[\text{dB}\right] = 10\log_{10}\left(1+\alpha_{\max}\right) = 10\log_{10}\left(1+10^{\frac{XPD_{\max}}{10}}\right) \quad (1.17)$$

where

$$XPD_{\max}[\text{dB}] = 10\log_{10}\left[\max\left(\left.\frac{P_{cross-pol}}{P_{co-pol}}\right|_{\text{P1},\gamma_{rot}=0^{\text{o}}}, \left.\frac{P_{cross-pol}}{P_{co-pol}}\right|_{\text{P1},\gamma_{rot}=90^{\text{o}}}, \ldots, \left.\frac{P_{cross-pol}}{P_{co-pol}}\right|_{\text{P7},\gamma_{rot}=0^{\text{o}}}, \left.\frac{P_{cross-pol}}{P_{co-pol}}\right|_{\text{P7},\gamma_{rot}=90^{\text{o}}}\right)\right] \quad (1.18)$$

C.13 Influence of TRP Measurement Grid

This contributor describes the uncertainty of the measured TRP value due to the finite number of measurement grid points.

C.14 Multiple Measurement Antennas

This contributor describes the uncertainty caused by switching multiple measurement antennas either mechanically or electrically.

C.15 DUT Repositioning

This contributor describes the uncertainty due to a misalignment of a DUT. The DUT may need to be re-oriented to avoid forming its beam toward the support structure during the measurement or when the device is placed back into the support structure after battery ran low in charge.

C.16 Influence of Spherical Coverage Grid

This contributor describes the uncertainty of spherical measurements, due to the finite number of measurement points in the spherical coverage grid.

C.17 Misalignment of Positioning System

This contribution originates from uncertainty in sliding position and turn table angle/tilt accuracy. If the calibration antenna is aligned to the beam peak this contribution can be considered negligible and therefore set to zero.

C.18 Network Analyzer

This contribution originates from all uncertainties involved in transmission magnitude measurement with a network analyzer, e.g., drift, frequency flatness, temperature variation from kit calibration to path losses measurement as well as interpolation of calibration data if test frequencies were not calibrated during path loss characterization. The uncertainty value will be indicated in the manufacturer's data sheet. It needs to be ensured that appropriate manufacturer's uncertainty contribution is specified for the settings (IF bandwidth, power levels, etc.) used.

When an end-to-end system calibration approach is used, the absolute levels are related to the total system losses of the measurement path. When a split calibration approach is used, separate MU contributions need to be determined

- u_cond: transmission magnitude uncertainty for the conducted portion of the calibration; the absolute levels are related to the total system losses for the portion of the system calibrated
- u_rad: transmission magnitude uncertainty for the radiated portion of the calibration; the absolute levels are related to the total system losses for the portion of the system calibrated

The total MU of the network analyzer for the split calibration is the RSS'ed value of u_cond and u_rad.

C.19 Absolute Gain of the Calibration Antenna

The calibration antenna only appears in the calibration stage where the gain uncertainty has to be taken into account. This uncertainty shall come from a calibration report with traceability to a National Metrology Institute with measurement uncertainty budgets generated following the guidelines outlined in internationally accepted standards.

C.20 Positioning and Pointing Misalignment between the Reference Antenna and the Measurement Antenna

This contribution originates from reference antenna alignment and pointing error. In this measurement if the maximum gain direction of the reference antenna and the transmitting antenna are aligned to each other, this contribution can be considered negligible and therefore set to zero.

C.21 Phase Center Offset of Calibration Antenna

Gain is defined at the phase center of the antenna. If the phase center of the calibration antenna is not aligned at the center of the set up during the calibration, then there will be uncertainty related to the measurement distance. For more information, see G.7.2 of [2].

For DFF systems this uncertainty contribution must be included while this term can be assumed to be zero inside the quiet zone for IFF systems.

C.22 Quality of Quiet Zone for Calibration Stage

During the calibration process the calibration antenna will be placed at the center of the quiet zone. Therefore, only point P1 from the quality of quiet zone procedure needs to be considered for the Quality of the Quiet Zone validation measurement.

C.23 Influence of the Calibration Antenna Feed Path

During the calibration measurement a cable (plus adapters, attenuators) is used to feed the calibration antenna. This uncertainty captures any influence the cable or miscellaneous components (adapters, attenuators, connector, and rotary joints) may have on the measurements result. This term can be assessed by repeating measurements while flexing the cables and rotary joints and using the largest difference between the results as the uncertainty.

C.24 Standing Wave between Reference Calibration Antenna and Measurement Antenna

This term comes from the amplitude ripple caused by the standing waves between the reference antenna and measurement antenna. This value can be captured by sliding (λ/4) the reference antenna towards the measurement antenna as the standing waves go in and out of phase causing a ripple in amplitude. The uncertainty term can be derived by performing the standard deviation on the results.

C.25 Insertion loss Variation

This uncertainty contribution comes from introducing an additional cable which is not present for both the calibration and DUT measurement. If the cables remain the same for the calibration and DUT measurement, then the contribution should be set to zero.

If an additional cable is added for one part of the test, the insertion loss must be accounted for in the measurement results. If the insertion loss is measured the uncertainty contribution will be the combined uncertainty related to the insertion loss measurement. The insertion loss can also be taken from the datasheet and assumed to have a rectangular distribution.

C.26 Influence of Noise

This contributor describes an offset uncertainty factor caused by a noise floor especially in a case of low SNR. This contributor works as a bias to measured results only to a direction to increase values and thus this shall be included in the uncertainty budget table as a systematic uncertainty. The uncertainty value can be derived by the following equation.

$$\text{Influence of noise} = 10 * \log_{10}\left(1 + 10^{\left(-\frac{SNR}{10}\right)}\right)$$

C.27 Systematic Error related to Beam Peak Search

When performing beam peak search measurements, a systematic error shall be taken into account. The value of this contributor depends on the number of measurement grid points.

This measurement uncertainty contributor represents a systematic uncertainty and must be added to the expanded uncertainty and not be root sum squared with contributors described by standard deviation.

C.28 Systematic Error Related to EIS Spherical Coverage

When calculating EIS spherical coverage, a mean error shall be taken into account. The value of this contributor depends on the DL power step size used for the EIS search and the number of measurement grid points.

This measurement uncertainty contributor represents a systematic uncertainty and must not be root sum squared with contributors described by standard deviation.

Appendix D Measurement Grids

Note: This test plan is currently applicable only to UE antennas with radiating aperture less than or equal to 5 cm. Measurement grids and measurement uncertainties for DUTs with antenna apertures greater than 5 cm have not been defined yet and can therefore not be certified using this test plan.

This appendix describes the measurement grids required for the TX Maximum Output Power (MOP) and RX Reference Sensitivity (REFSENS) test cases in this test plan. A total of three measurement grids are required for all tests:

- Beam Peak Search Grid: using this grid, the TX and RX beam peak direction will be determined. 3D EIRP scans are used to determine the TX beam peak direction and 3D Throughput/EIS scans for RX beam peak directions.
- Spherical Coverage Grid: using this grid, the CDF (CCDF) of the EIRP (EIS) distribution in 3D is calculated to determine the spherical coverage performance.
- TRP Measurement Grid: using this grid, the total power radiated by the DUT in the TX beam peak direction is determined by integrating the EIRP measurements taken on the sampling grid.

The UE antenna assumptions and measurement grid simulations are summarized in detail in [1]. The relevant measurement grid guidelines in terms of minimum number of grid points, grid types, and implementations, are provided in this appendix.

D.1 Grid Types

Two different measurement grid types are considered. The constant step size grid type has the azimuth and elevation angles uniformly distributed as illustrated in in 2D Figure D.1-1 and Figure D.1-2 in 3D and matches the measurement grid in [2].

Figure D.1-1 Sample Distribution of Measurement Grid Points in 2D for a Constant Step Size Grid with $\Delta\theta=\Delta\phi=15^{o}$ (266 Unique Measurement Points)

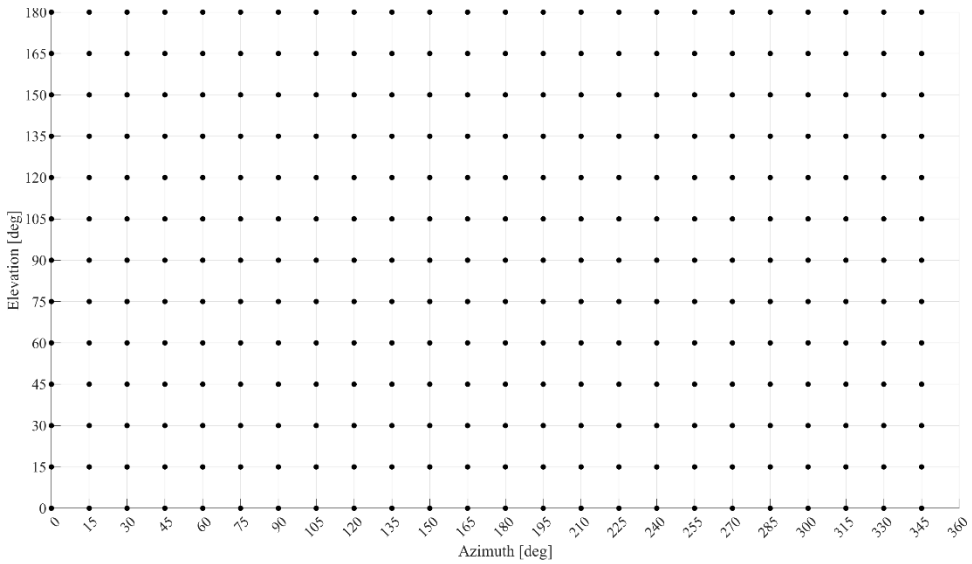

Figure D.1-2 Sample Distribution of Measurement Grid Points in 3D for a Constant Step Size Grid with $\Delta\theta=\Delta\phi=15^{o}$ (266 Unique Measurement Points)

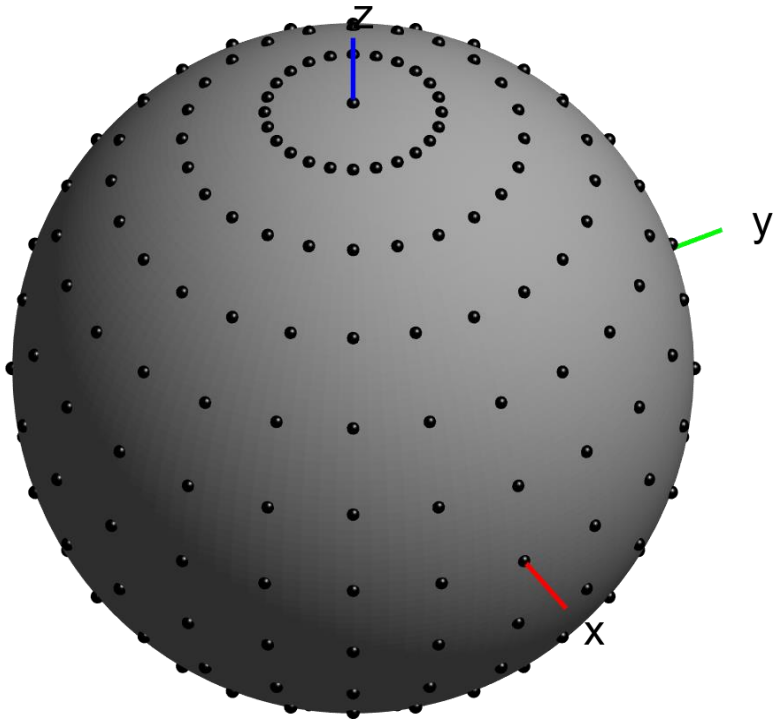

Constant density grid types have measurement points that are evenly distributed on the surface of the sphere with a constant density as illustrated in Figure D.1-3 in 2D and Figure D.1-4 in 3D.

The best implementation of the constant density grid was shown to be based on the charged particle approach [3] where the resulting grid points produce a minimum energy configuration of equally charged particles confined to the surface of a unit sphere. A suitable Matlab implementation can be found in [4]. This measurement grid implementation is an improvement when compared to the theta dependent phi step size optimization in [2].

Figure D.1-3 Sample Distribution of Measurement Grid Points in 2D for a Constant Density Grid with 266 Unique Measurement Points

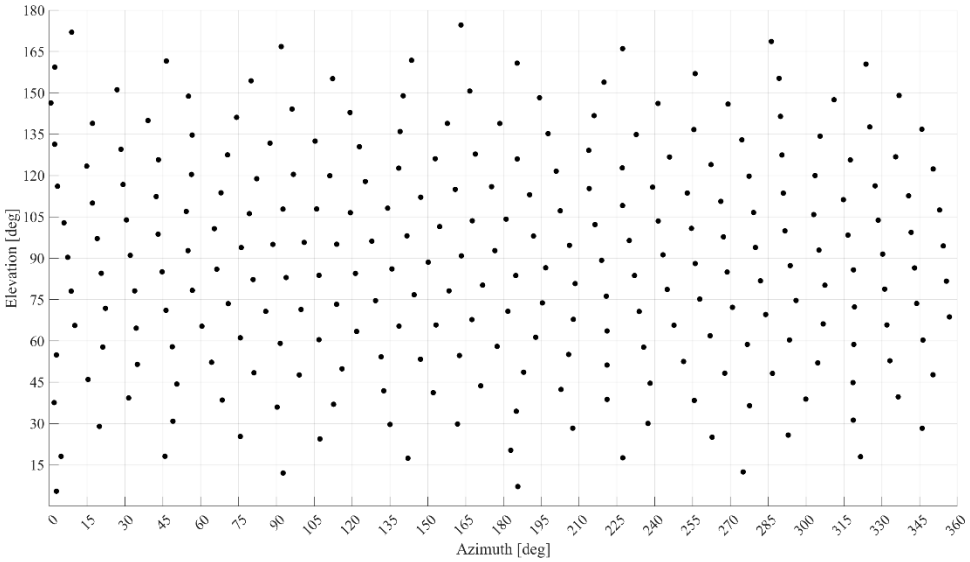

Figure D.1-4 Sample Distribution of Measurement Grid Points in 3D for a Constant Density Grid Type with 266 Unique Measurement Points

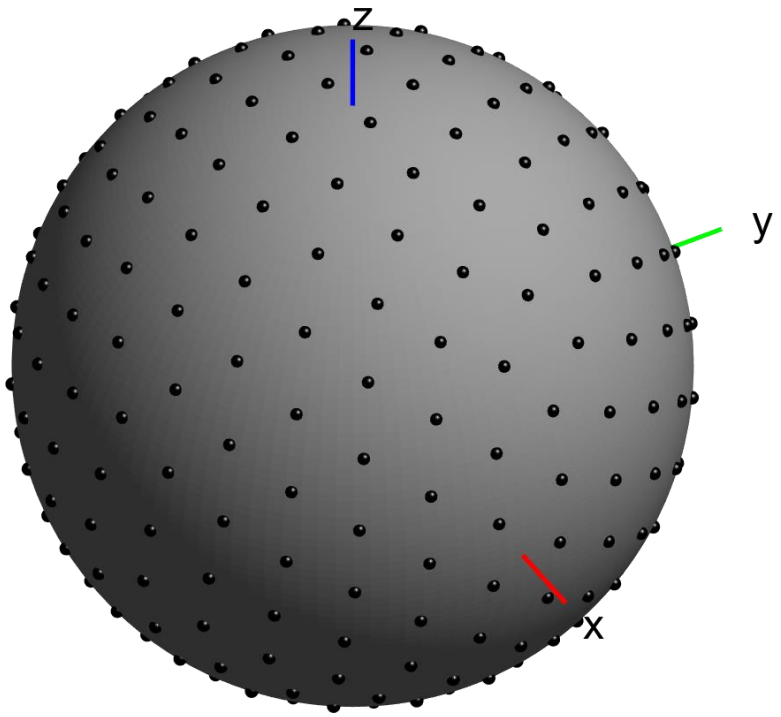

The choice of the two grid types, constant step size vs constant density using the charged particle approach, is up to test system vendors.

D.2 TRP Measurement Grids

This sub-section outlines the requirements of the TRP measurement grids for the two grid types. In many engineering disciplines, the integral of a function needs to be solved using numerical integration techniques, commonly referred to as “quadrature”. Here, the approximation of the integral of a function is usually stated as a weighted sum of function values at specified points within the domain of integration. The transformation from the closed surface TRP integral:

$$\text{TRP} = \oiint_S \text{EIRP}(\theta, \phi) \cdot d\Omega$$

to discretized summation equations has been solved various ways.

For constant step size grids, the most optimized approach in terms of measurement uncertainty was shown to be based on the Clenshaw-Curtis quadrature integral approximation based on an expansion of the integrand in terms of Chebyshev polynomials [5][6].This implementation does not ignore the measurement points at the poles (θ=0º and 180º) where sin(θ) = 0 when compared to the classical OTA quadrature based on the sin(θ) $\Delta\theta$ weights [2].The discretized TRP can be expressed as

$$\text{TRP} \approx \frac{1}{2M} \sum_{i=0}^{N} \sum_{j=0}^{M-1} \left[\text{EIRP}_{\theta}(\theta_i, \phi_j) + \text{EIRP}_{\phi}(\theta_i, \phi_j)\right] \text{W}(\theta_i)$$

with the weight function $\text{W}(\theta)$. The TRP measurement grid consists of N+1 latitudes and M longitudes with:

$$\theta_i = i\Delta\theta \text{ where } \Delta\theta = \frac{\pi}{N}$$

And:

$$\phi_j = j\Delta\phi \text{ where } \Delta\phi = \frac{2\pi}{M}$$

There is no simple closed-form expression for the Clenshaw-Curtis weights; however, a numerical straightforward approach is available in [7], i.e.

$$W(\theta_i) = \frac{c_i}{N}\left[1 - \sum_{j=1}^{\text{int}(\frac{N}{2})} \frac{b_j}{4j^2 - 1} \cos(2j\theta_i)\right]$$

With:

$$b_j = \begin{cases} 1, & 2j = N \\ 2, & otherwise \end{cases}$$

and

$$c_i = \begin{cases} 1, & i = 0 \text{ or } N \\ 2, & otherwise \end{cases}$$

The Clenshaw-Curtis weights are tabulated in Table D.2.1 and Table D.2-2 for two different numbers of latitudes that were found to yield a standard deviation of less than 0.25 dB for the UE antenna assumptions outlined in [1].

Table D.2.1 Samples and Weights for the Clenshaw-Curtis Quadrature with 12 Latitudes ($\Delta\theta=\pi/11$)

Clenshaw-Curtis	
θ [°]	**Weights**
0	0.0083
16.4	0.0786
32.7	0.1550
49.1	0.2156
65.5	0.2599
81.8	0.2827
98.2	0.2827
114.6	0.2599
130.9	0.2156
147.3	0.1550
163.6	0.0786
180	0.0083

Table D.2-2 Samples and Weights for the Clenshaw-Curtis Quadrature with 13 Latitudes ($\Delta\theta$=15°)

Clenshaw-Curtis	
θ [°]	Weights
0	0.0070
15	0.0661
30	0.1315
45	0.1848
60	0.2270
75	0.2527
90	0.2620
105	0.2527
120	0.2270
135	0.1848
150	0.1315
165	0.0661
180	0.0070

For constant density grid types using the charged particle approach, the TRP integration should ideally take into account the area of the Voronoi region [8] surrounding each grid point. Assuming an ideal constant density configuration of the grid points, the TRP can be approximated using

$$\mathrm{TRP} \approx \frac{1}{N}\sum_{i=0}^{N-1}\left[\mathrm{EIRP}_{\theta}(\theta_i,\phi_i) + \mathrm{EIRP}_{\phi}(\theta_i,\phi_i)\right]$$

As illustrated in Figure D.2-1, for systems that either do not allow measurements at the pole (θ=180°), e.g., using distributed-axes positioners, or systems that have the positioners/support structures block the radiation towards the pole (θ=180°), e.g., combined-axes positioners, the measurements in the region close to the pole at θ=180° can be skipped and interpolated instead.

Figure D.2-1 Illustration of Areas Around the Pole that Either Cannot be Reached by the Measurement Antenna or are Blocked by the Positioner

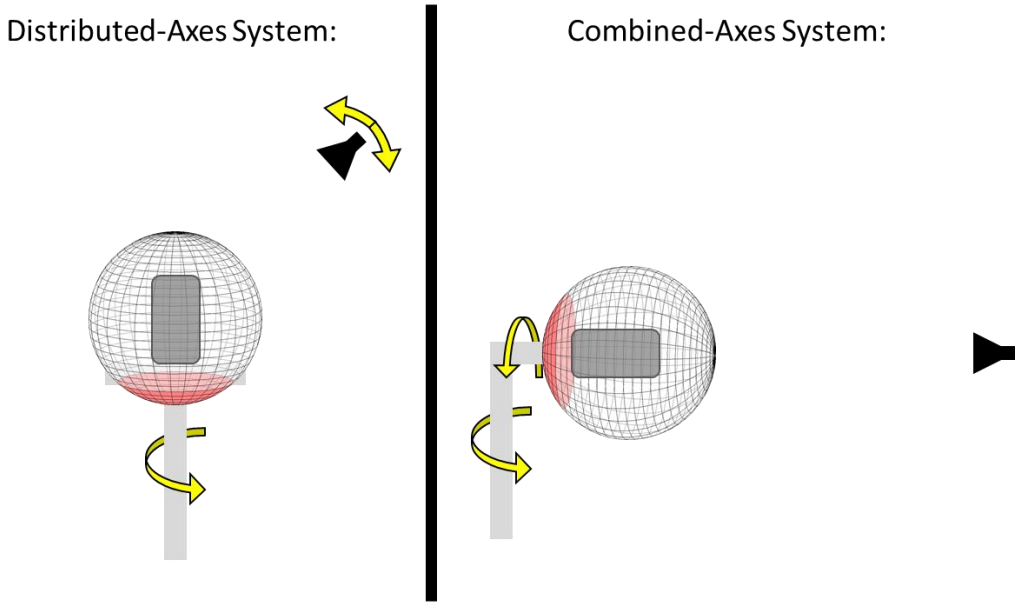

The results tabulated in the tables below outline the results of a statistical analyses for the 8x2 antenna array [1] while taking into account the positioning concept, i.e., the analyses were performed with the assumption that the beam peak direction is oriented away from the hemisphere towards the pole at $\theta=180^{o}$. Additionally, the standard deviations are presented when ranges of pattern values are disregarded (zeroed out). For the constant-step size measurement grids, three cases were investigated, i.e., no pattern values are disregarded, values only at one latitude at $\theta=180^{o}$, and the values at the bottom two latitudes are disregarded. For the constant density measurement grids, a similar investigation was performed using the Charged Particle implementation. Since there are no latitudes defined, the three cases investigated were: no pattern values are disregarded, values between $165^{o}\leq\theta\leq180^{o}$, and values between $150^{o}\leq\theta\leq180^{o}$ are disregarded.

These results clearly show that for the measurement grids proposed in Appendix D.1 and with the re-positioning concept considered, the measurements beyond 165^{o} in θ can be skipped and interpolated instead. Alternate measurement grids listed in the tables below with larger number of grid points are not precluded where the measurements beyond 150^{o} in θ can be skipped and interpolated instead provided that the standard deviation of 0.25 dB is met.

Table D.2-3 Statistics of Quadrature Approaches for Constant Step Size Measurement Grids for the 8x2 Reference Antenna Array

Number Of		Number of Latitudes Disregarded	Mean Error [dB]	STD. DEV [dB]	Min TRP Error [dB]	Max TRP Error [dB]	Quadrature	Re-Positioning Concept Applied
Latitudes	Longitudes							
13	24	0	0.00	0.06	-0.23	0.21	Clenshaw-Curtis	Yes
13	24	1	-0.01	0.07	-0.34	0.21	Clenshaw-Curtis	Yes
13	24	2	-0.08	0.15	-0.78	0.19	Clenshaw-Curtis	Yes
12	19	0	0.00	0.20	-0.97	0.76	Clenshaw-Curtis	Yes
12	19	1	-0.01	0.21	-0.94	0.77	Clenshaw-Curtis	Yes
12	19	2	-0.10	0.26	-0.96	0.77	Clenshaw-Curtis	Yes

Table D.2-4 Statistics for Constant Density Measurement Grid Types for the 8x2 Reference Antenna Array (Charged Particle Implementation Only)

Number Of Grid Points	Range of Angles Disregarded	Mean Error [dB]	STD. Dev [dB]	Min TRP Error [dB]	Max TRP Error [dB]	Re-Positioning Concept Applied
130	none	0.00	0.27	-0.95	0.81	yes
135	none	-0.01	0.22	-0.84	0.71	yes
140	none	0.00	0.19	-0.75	0.68	yes
145	none	-0.01	0.19	-0.61	0.58	yes
150	none	0.00	0.15	-0.60	0.53	yes
155	none	0.00	0.13	-0.42	0.52	yes
160	none	0.00	0.11	-0.41	0.43	yes
165	none	0.00	0.09	-0.40	0.39	yes
170	none	0.00	0.08	-0.36	0.37	yes
175	none	0.00	0.06	-0.27	0.29	yes
130	165°-180°	-0.05	0.29	-1.20	0.77	yes

Number Of Grid Points	Range of Angles Disregarded	Mean Error [dB]	STD. Dev [dB]	Min TRP Error [dB]	Max TRP Error [dB]	Re-Positioning Concept Applied
135	165°-180°	-0.03	0.23	-1.18	0.67	yes
140	165°-180°	-0.05	0.22	-0.94	0.70	yes
145	165°-180°	-0.02	0.19	-0.82	0.57	yes
150	165°-180°	-0.03	0.16	-0.84	0.56	yes
155	165°-180°	-0.04	0.15	-0.74	0.48	yes
160	165°-180°	-0.04	0.13	-0.75	0.43	yes
165	165°-180°	-0.04	0.12	-0.71	0.36	yes
170	165°-180°	-0.04	0.12	-0.58	0.34	yes
175	165°-180°	-0.04	0.10	-0.65	0.27	yes
130	150°-180°	-0.16	0.35	-1.77	0.73	yes
135	150°-180°	-0.15	0.31	-1.93	0.63	yes
140	150°-180°	-0.18	0.30	-1.55	0.57	yes
145	150°-180°	-0.14	0.28	-1.29	0.54	yes
150	150°-180°	-0.15	0.25	-1.26	0.53	yes
155	150°-180°	-0.13	0.23	-1.09	0.46	yes
160	150°-180°	-0.16	0.24	-1.15	0.42	yes
165	150°-180°	-0.16	0.24	-1.12	0.32	yes
170	150°-180°	-0.15	0.23	-0.99	0.30	yes
175	150°-180°	-0.13	0.20	-0.90	0.28	yes

For Power Class 3 devices with radiating apertures of less than or equal to 5 cm, i.e., non-sparse antenna arrays, either of the following measurement grids and implementations were found to be the best trade-off between measurement uncertainties, measurement grid points, and test time. Either of the choices shall be used for this test plan:

- At least 135 measurement grid points for the constant density grid using the Charged Particle implementation with a standard deviation of 0.23 dB with the allowance to skip and interpolate measurements beyond 165° in θ
- At least 150 measurement grid points for the constant density grid using the Charged Particle implementation with a standard deviation of 0.25 dB with the allowance to skip and interpolate measurements beyond 150° in θ

- At least 192 unique measurement grid points (12 latitudes and 19 longitudes) for constant step size grid using the Clenshaw Curtis quadrature with standard deviation of 0.21 dB with the allowance to skip and interpolate measurements the at pole at $\theta=180^{o}$
- At least 266 unique measurement grid points (13 latitudes and 24 longitudes) for constant step size grid using the Clenshaw Curtis quadrature with standard deviation of 0.15 dB with the allowance to skip and interpolate measurements beyond 150^{o} in θ

D.3 Beam Peak Search Measurement Grids

The beam peak search grid is used to determine the beam peak of the TX and RX beams.

For Power Class 3 devices with radiating apertures of less than or equal to 5 cm, i.e., non-sparse antenna arrays, either of the following measurement grids and implementations were found to be the best trade-off between measurement uncertainties, measurement grid points, and test time. Either of the two choices shall be used for this test plan:

- At least 800 measurement grid points for the constant density grid using the charged particle implementation
- At least 1106 measurement grid points (angular step size of 7.5^{o}) for the constant step size grid

The corresponding systematic error related to Beam Peak Search is 0.5 dB for the above choices.

D.4 Spherical Coverage Measurement Grids

The spherical coverage measurement grid is used to determine the CDF (CCDF) curve for EIRPs (EISs) measured on each grid point. For constant step size measurement grid types, the PDF probability contribution for each measurement point is scaled by the normalized Clenshaw-Curtis weights $W(\theta)/W(\theta=90^{o})$ as outlined in Appendix D.2 to account for the denser grid point distribution near the poles. Due to the constant density nature of the constant density grids, this correction is not needed for these grid types.

For Power Class 3 devices with radiating apertures of less than or equal to 5 cm, i.e., non-sparse antenna arrays, either of the following measurement grids and implementations were found to be the best trade-off between measurement uncertainties, measurement grid points, and test time. Either of the two choices shall be used for this test plan:

- At least 200 measurement points for the constant density grid using the charged particle implementation with a standard deviation of 0.11 dB
- At least 266 unique measurement grid points (angular step size of 15^{o}) constant step size grid with a standard deviation of 0.12 dB

For EIS spherical coverage, an additional systematic error needs to be included in the measurement uncertainty budget that matches the DL power step size for the final EIS search.

The spherical coverage measurements can be performed without having to have the beam peak placed on a grid point, i.e., the beam peak does not need to be known prior to performing the spherical coverage test cases.

D.4.1 Clarification of Min EIRP/Max EIS at Target CDF/CCDF Value

When CDF/CCDF curves are generated based on spherical coverage measurement grids instead of beam peak search measurements grids, the number of non-zero PDF values could be very limited which

causes the CDF curve to appear staggered. One sample, simulated CDF curve is shown in Figure D.4.1-1 for a coarse measurement grid.

Figure D.4.1-1 Sample CDF Curve for a Coarse Measurement Grid

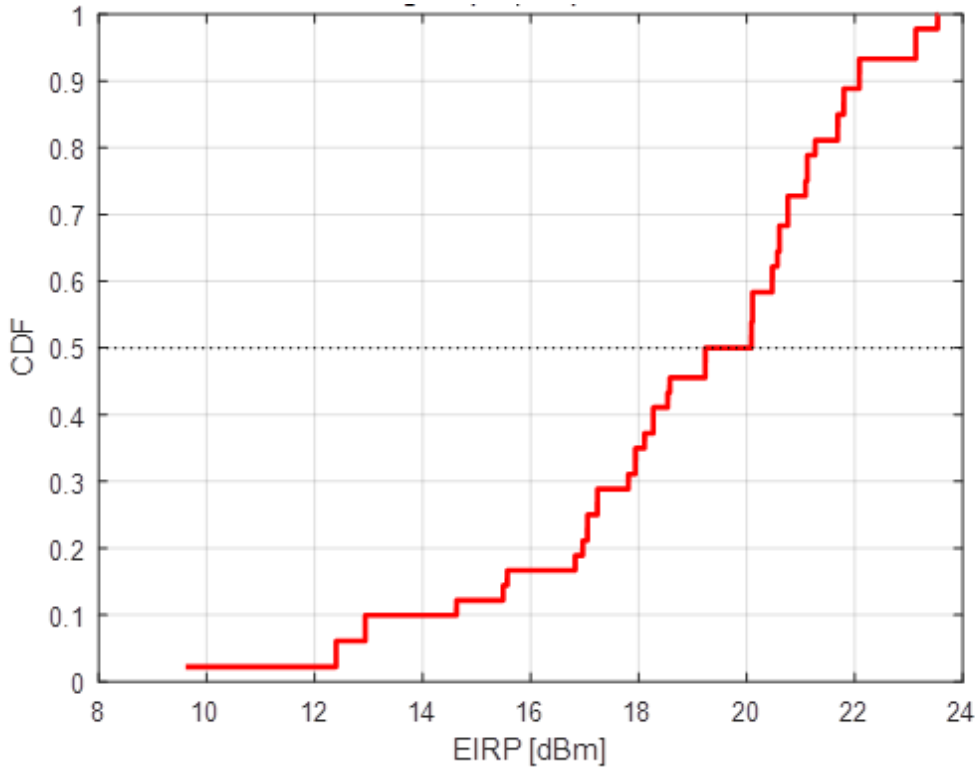

While for very fine measurement grids, the definition of the min EIRP (max EIS) at the 50% CDF (CCDF), $EIRP_{50\%\text{-}CDF}$ ($EIS_{50\%\text{-}CCDF}$), is pretty clear since the CDF (CCDF) curve is smooth, the definition of the EIRP (EIS) value at the respective CDF (CCDF) target should be clarified for coarse grids with staggered CDF (CCDF) curves. Two scenarios are outlined in Figure D.4.1-2 for EIRP; the concept can easily be applied to EIS. Figure D.4.1-2a shows the case where the CDF is not met with any EIRP value while in Figure D.4.1-2b, the target CDF is met with one (or more, as illustrated) EIRP values.

For the case shown in Figure D.4.1-2a, min. EIRP at the target CDF shall be determined based on an interpolation of the CDF curve between the top of raising edges located right above the CDF target (blue circle) and right below the target (green circle).

For the case where the target CDF is met with one or more EIRP value(s), as illustrated in Figure D.4.1-2b, min EIRP at the target CDF shall be determined as the min EIRP value that meets the CDF target.

Figure D.4.1-2: Illustration of CDF Scenarios, a) CDF Target is Not Met with any EIRP Value, b) CDF Target Is Met with One or more EIRP Values

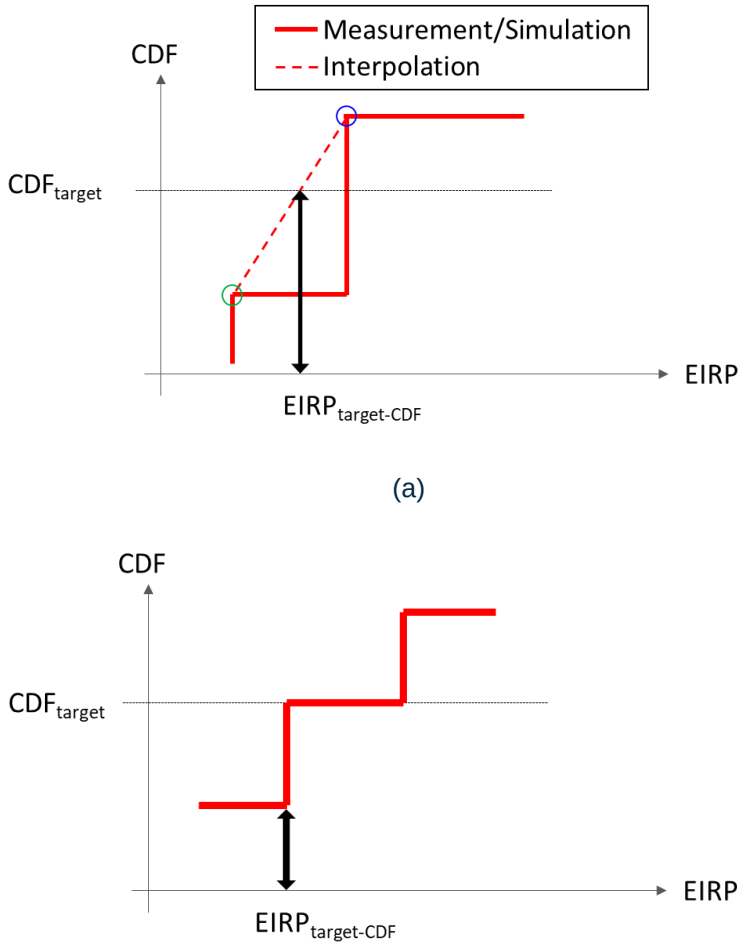

It can be concluded that, for the case when the target CDF (CCDF) is not met with any EIRP (EIS) values, the min EIRP (max EIS) at the target CDF (CCDF) is determined based on an interpolation of the CDF (CCDF) curve between the raising edges located right above the CDF (CCDF) target and right below the target. For the case where the target CDF (CCDF) is met with one more or EIRP (EIS) values, define the min EIRP (max EIS) at the target CDF (CCDF) as the min EIRP (max EIS) value that meets the CDF (CCDF) target.

Appendix E Reporting of Test Results (Normative)

E.1 Introduction

Test reports and files shall be provided as described in this section. Deliverables consist of a Range Reference Measurement data file (Section 4) and DUT Measurement data files (as described in this section) for each DUT characterized.

DUT and results shall be reported in various ways:

- A complete set of the documentation on the DUTs tested and the respective test conditions
- A complete set of the measurement data for every test supplied electronically in a format that can be easily read (e.g., Excel, etc.) using the table templates in this appendix
- A complete set of summary report for every test using the table templates in this appendix
- 3D plots for the MOP-TRP measurement in the mid test frequency range CDF/CCDF plots for the TX and RX spherical coverage test cases, respectively

See Section 1.5 of the CTIA OTA test plan [2] for addition details. The remaining sections list the required report tables and templates.

E.2 Report Tables Related to DUT(s)

Table E.2-1: DUT Information Device Under Test (DUT) Information

Device Under Test (DUT) Information	
Manufacturer	
Model	
Serial Number(s)/ESN(s)/IMEI(s)	
FCC ID Number	
Hardware Version	
Software Version	
Configuration of Primary Mechanical Mode	

Table E.2-2: Bands and Protocols Supported by DUT

NR Bands	**LTE Bands**

E.3 Report Result Tables for TX

Table E.3-1: TX Beam Peak Search

EUT θ [°]	EUT ϕ [°]	DL Polarization (POL_{LINK})	NR Band	BW/SCS	UL/DL Frequency [MHz]	Testing Condition	EIRP (POL_{MEAS}=θ) [dBm]	EIRP (POL_{MEAS}=ϕ) [dBm]	EIRP [dBm]

Table E.3-2: TX Beam Peak Search Summary

DUT θ [°]	DUT ϕ [°]	DL Polarization (POLLINK)	NR Band	BW/SCS	UL/DL Frequency [MHz]	Testing Condition	EIRP [dBm]

Table E.3-3: MOP-EIRP Summary

DUT θ [°]	DUT ϕ [°]	DL Polarization (POL_{LINK})	NR Band	BW/SCS	UL/DL Frequency [MHz]	Testing Condition	EIRP [dBm]

Table E.3-4: MOP-TRP Results

DUT θ [°]	DUT ϕ [°]	DL Polarization (POL_{LINK})	NR Band	BW/SCS	UL/DL Frequency [MHz]	Testing Condition	EIRP (POL_{MEAS}=θ) [dBm]	EIRP (POL_{MEAS}=ϕ) [dBm]	EIRP [dBm]

Table E.3-5: MOP-TRP Summary

DUT θ [°]	DUT ϕ [°]	DL Polarization (POL_{LINK})	NR Band	BW/SCS	UL/DL Frequency [MHz]	Testing Condition	TRP [dBm]

Table E.3-6: MOP-Spherical Coverage Results

DUT θ [°]	DUT ϕ [°]	DL Polarization (POL_{LINK})	NR Band	BW/SCS	UL/DL Frequency [MHz]	Testing Condition	EIRP (POL_{MEAS}=θ) [dBm]	EIRP (POL_{MEAS}=ϕ) [dBm]	EIRP [dBm]

Table E.3-7: MOP-Spherical Coverage CDF Results

NR Band	BW/SCS	UL/DL Frequency [MHz]	Testing Condition	EIRP [dBm]	CDF [%]

Table E.3-8: MOP-Spherical Coverage CDF Summary

NR Band	BW/SCS	UL/DL Frequency [MHz]	Testing Condition	Testing Condition	$EIRP_{50\%CDF}$ [dBm]

E.4 Report Result Tables for RX

Table E.4-1: RX Beam Peak Search

DUT θ [°]	DUT ϕ [°]	DL Polarization (POL_{LINK})	NR BAND	BW/SCS	UL/DL Frequency [MHz]	Testing Condition	EIS (POL_{MEAS}= POL_{LINK}) [dBm]

Table E.4-2: RX Beam Peak Search Summary

DUT θ [°]	DUT ϕ [°]	NR Band	BW/SCS	UL/DL Frequency [MHz]	Testing Condition	EIS_{AVG} [dBm]

Table E.4-3: REFSENS-EIS Summary

DUT θ [°]	DUT ϕ [°]	NR Band	BW/SCS	UL/DL Frequency [MHz]	Testing Condition	EIS_{AVG} [dBm]

Table E.4-4: REFSENS-Spherical Coverage Results

DUT θ [°]	DUT ϕ [°]	DL Polarization (POL_{LINK})	NR Band	BW/SCS	UL/DL Frequency [MHz]	Testing Condition	EIS (POL_{MEAS}=POL_{LINK}) [dBm]

Table E.4-5: REFSENS-Spherical Coverage CCDF Results

NR Band	BW/SCS	UL/DL Frequency [MHz]	Testing Condition	EIS_{AVG} [dBm]	CCDF [%]

Table E.4-6: REFSENS-Spherical Coverage CCDF Summary

NR Band	BW/SCS	UL/DL Frequency [MHz]	Testing Condition	$EIS_{50\%CCDF}$ [dBm]

Table E.2-3: DUTs Used for Each Test

Serial Number/ ESN/IMEI	CATL and Chamber Used	NR Band(S)	LTE Band	Test Type(s)	Test Condition(s), e.g., Alignment Options/DUT Orientations, etc.

Appendix F Phase Quality of Quiet Zone Procedure

This appendix outlines the test procedures to evaluate the phase variation within the quiet zone. Either the rotary scan procedure in F.4 or the field probing procedure in F.5 can be used to determine the largest phase variation.

F.1 Minimum Measurement Distance

The quality of quiet zone validation shall be performed in the far-field distance of the UE antennas.

F.2 Equipment Required

The reference Antenna Under Test (AUT) that is placed at various locations within the quiet zone shall be a directive antenna with similar properties of typical antenna arrays integrated in DUTs. The characteristics in terms of Directivity and Half Power Beamwidth (HPBW) of the reference AUT are the same as Section 3.2.

For the measurement, a network analyzer can be used. The multi-port (with three ports) network analyzer is most suitable to reduce test time as both polarizations of the measurement antenna can be measured simultaneously, and multiple frequencies can be measured in a sweep.

F.3 Test Frequencies

The Quality of Quiet Zone test frequencies are the same as those outlined in Section 3.3 the amplitude quality of quiet zone testing.

F.4 Rotary Scan Procedure

With this approach, the phase behavior is characterized on multiple points on a circular trajectory within the quiet zone as illustrated in Figure F.4-1.

Figure F.4-1 Characterization of the Phase Response Within the Quiet Zone using a Rotary Scan

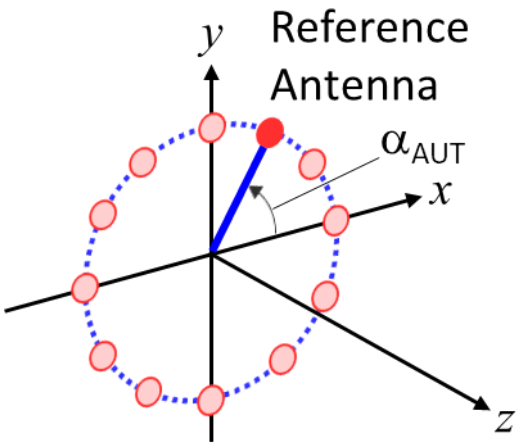

This measurement can be accomplished using a reference AUT connected to the end of a rotary arm scanning the circular path centered on the center of the quiet zone. Such a rotary movement can capture all of the impact on phase as in actual test cases since it uses the same positioning equipment used for such tests. For these scans, the reference AUT is directed towards the z axis and the rotary scan is performed within the x and y plane. For this test, a reference antenna with single polarization is sufficient

but two orthogonal polarizations shall be tested, as outlined in Figure F.4-2 for the reference antenna starting out in the H-Polarization (principal polarization aligned with x axis) and in Figure F.4-3 for the reference antenna starting out in the V-polarization (principal polarization aligned with y axis) at rotary angle, α_{AUT}, of 0°.

Figure F.4-2 Sample reference AUT positions with starting H-polarization of rotary angle α_{AUT} = 0°

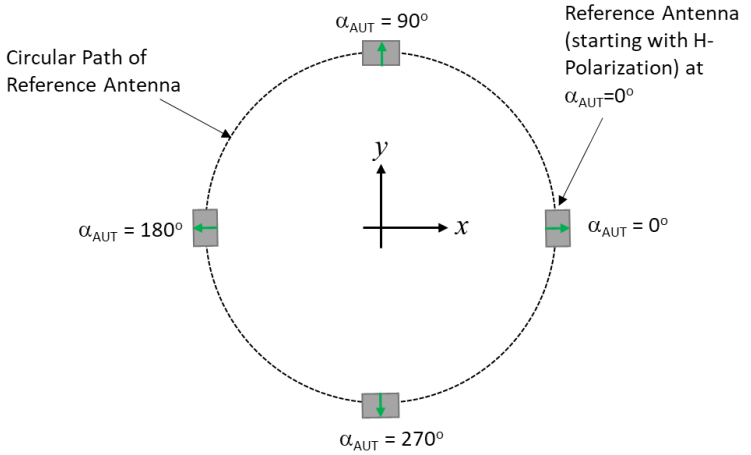

Figure F.4-3 Sample reference AUT positions with starting V-polarization of rotary angle α_{AUT} = 0°

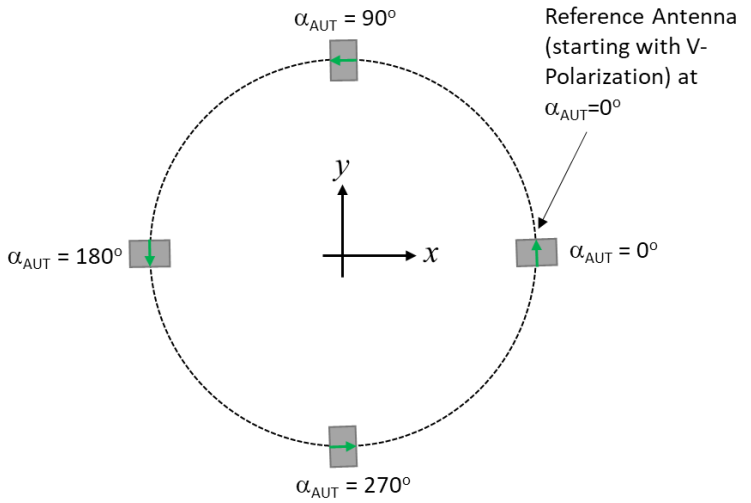

Due to cross-polarization effects between the reference antenna and the feed antenna, e.g., the measurement is in a null for the H-Pol feed/measurement antenna when the reference antenna is at rotary angles 90° and 270° of Figure F.4-2, the phases shall be measured at the H and V polarized ports of the feed/measurement antenna as a function of the rotary angle α_{AUT}. As illustrated in Figure F.4-2 and Figure F.4-3, the phase jumps by 180° for sets of reference AUT positions that are opposite from each other, which needs to be compensated in post-processing of the phase measurements. If the path loss calibration was performed without the phase, i.e., without full two-port calibration on both polarizations, a phase alignment between the H and V measurements is necessary to eliminate the fixed phase offset between both measurement paths, e.g., by performing phase measurements at rotary angle of α_{AUT} = 45°. The two separate phase measurements can be combined into one curve by calculating the overall phase of the phasor, i.e.,

$$\beta = \angle\left[S_{1H}\cos(\alpha_{AUT}) + S_{1V}\sin(\alpha_{AUT})\right] \quad \text{(EQUATION F.1)}$$

for the test when the reference AUT starts out with an H-polarization at of α_{AUT} = 0º, see Figure F.4-2, and

$$\beta = \angle\left[S_{1V}\cos(\alpha_{AUT}) + S_{1H}\sin(\alpha_{AUT})\right] \quad \text{(EQUATION F.2)}$$

for the test when the reference AUT starts out with a V-polarization at of α_{AUT} = 0º, see Figure F.4-3.

Here, β is the resulting phase variation on circular path while S_{1H} (S_{1V}) are the S-parameter measured at the H (V) port of the feed/measurement antenna and $\angle$ is the operator for the phase.

This procedure shall be performed at four fixed radii of R=15 cm, 10 cm, 5 cm, and 0 cm at z=0 as illustrated schematically in Figure F-4.4. Additionally, rotary scans at R=0 cm and the perimeter of the spherical quiet zone at offsets in ±z shall be evaluated, i.e., one rotary scan with 5 cm radius at z=±14.15 cm, as illustrated in Figure F-4.5. Each rotary scan shall be performed for rotary angle increments of every 0.5º.

Figure F-4.4 Rotary Scan at Four Fixed Radii at z=0.

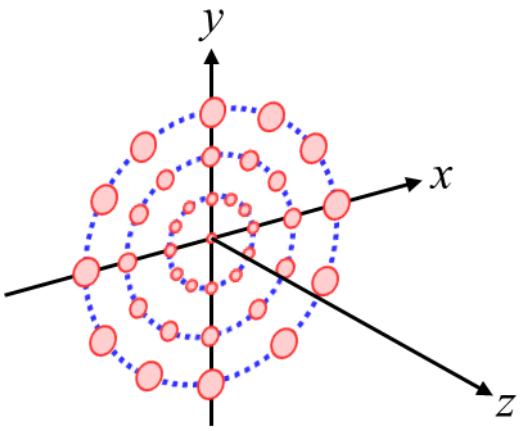

Figure F-4.5 Rotary Scans Within Spherical Quiet Zone

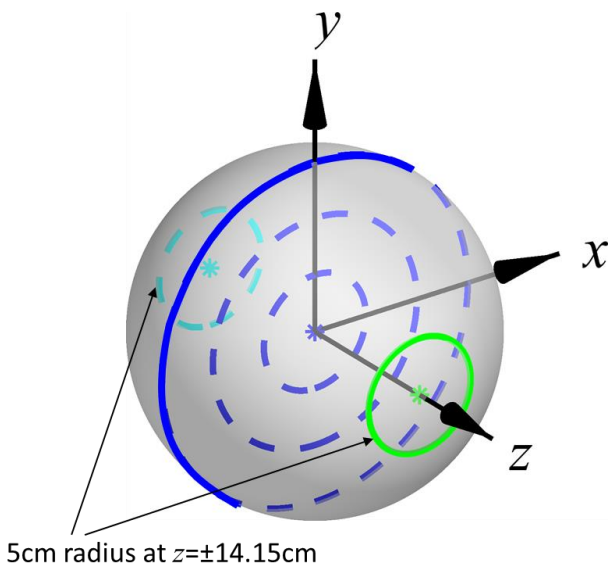

The basic measurement procedure is therefore as follows:

1. Mount the reference AUT at fixed radius R=15 cm at z=0.
2. Align the principal polarization of the reference AUT with the x-axis (horizontal) at rotary angle α_{AUT} = 0° (see Figure F.4-2) with the antenna facing the z direction.
3. Perform S_{1H} and S_{1V} measurements every 0.5° in rotary angle α_{AUT} for each test frequency outlined in Section 3.3.
4. Calculate the resulting phase variation on the circular path of radius R using Equation F.1 and Equation F.2.
5. Align the principal polarization of the reference AUT with the y-axis (vertical) at rotary angle α_{AUT} = 0° (see Figure F.4-3) with the antenna facing the z direction.
6. Perform S_{1H} and S_{1V} phase measurements every 0.5° in rotary angle α_{AUT} for each test frequency outlined in Appendix F.3.
7. Calculate the resulting phase variation on the circular path of radius R using Equation F.2.
8. Mount the reference AUT at fixed R=10 cm and repeat steps 2 through 7 and subsequently move to step 9.
9. Mount the reference AUT at fixed R=5 cm and repeat steps 2 through 7 and subsequently move to step 10.
10. Mount the reference AUT at fixed R=0 cm and repeat steps 2 through 7 and subsequently move to step 11.
11. Move the reference AUT at fixed radius R=0 cm at z=+14.15 cm and repeat step 2 through 7 and subsequently move to step 12.
12. Move the reference AUT at fixed radius R=5 cm at z=+14.15 cm and repeat step 2 through 7 and subsequently move to step 13.
13. Move the reference AUT at fixed radius R=0 cm at z=-14.15 cm and repeat step 2 through 7 and subsequently move to step 14.

14. Move the reference AUT at fixed radius R=5 cm at z=-14.15 cm and repeat step 2 through 7.

Alternatively, the use of a dual-polarized reference AUT is not precluded and a slightly modified procedure could be used.

The phase variations shall be evaluated for the combined rotary scans independently for each constant z, i.e., the phase variation due to the propagation in the z-direction shall not be compensated. The maximum phase variation for each fixed z is determined by combining (concatenating) all radial scans performed at given z, e.g., R={15 cm, 10 cm, 5 cm, 0 cm} at z=0, and evaluating the total peak-to-peak variation. The maximum phase variation within the spherical quiet zone, $\Delta\beta_{\max}$, shall be calculated and reported using:

$$\Delta\beta_{\max} = \max\begin{bmatrix} \Delta\beta(R=\{15\text{cm},\ 10\text{cm},\ 5\text{cm},\ 0\text{cm}\}, z=0), \Delta\beta(R=\{5\text{cm},\ 0\text{cm}\}, z=-14.15\text{cm}), \\ \Delta\beta(R=\{5\text{cm},\ 0\text{cm}\}, z=14.15\text{cm}) \end{bmatrix}$$

(EQUATION F.3)

where $\Delta\beta$ is the maximum phase variation within concatenated rotary scans performed at position z, i.e.,

$$\Delta\beta(R,z) = \max\left[\beta(R,z)\right] - \min\left[\beta(R,z)\right] \qquad \text{(EQUATION F.4)}$$

Note that it is necessary to unwrap the phase if any β has rolled over a 360° boundary, e.g. -180° to +180°.

F.5 Field Probing Procedure

The phase variation is determined from a phase probe trace by measuring the full excursion of the phase over the aperture of the quiet zone and is recorded in degrees.

Any positioners and/or support structures used throughout any conformance tests shall be installed in the system, i.e., the DUT positioner shall not be removed and its impact on the phase variation shall be taken into account.

The outcome of the procedures can be used to predict the variation of phase of the synthesized plane wave in the quiet zone. The reference coordinate system defined in Appendix C applies to this procedure.

Evaluation of the IFF quiet zone is accomplished by directly sampling the phase characteristics of the quiet zone field using the antenna specified in Section 3.2 as reference antenna. The reference antenna is placed at various locations within the quiet zone and analysis of the data reveals the field phase variations as a function of frequency and quiet zone location.

The reference AUT is attached to a linear rail placed at the range centerline height at the front, middle and rear of the quiet zone. Field samples are collected as the antenna is scanned horizontally, vertically, and along +45° and -45° paths. In all scans, both polarizations [V, H] shall be measured.

The reference positions are shown in Figure F.5-1. The phase shall be recorded in the xy plane, in increments of $\lambda/2$ or smaller for all positions that are contained within the spherical quiet zone at three different positions in z, i.e., within a circle of radius R=15 cm at z= 0, and within a circle of radius R=5 cm at z=±14.15 cm. A calibration is performed for both polarizations at each z position, at x, y = 0 (0,0,z). This in effect makes each point measured in r relative to (0,0,z).

Figure F.5-1: Field Probing – Reference Positions

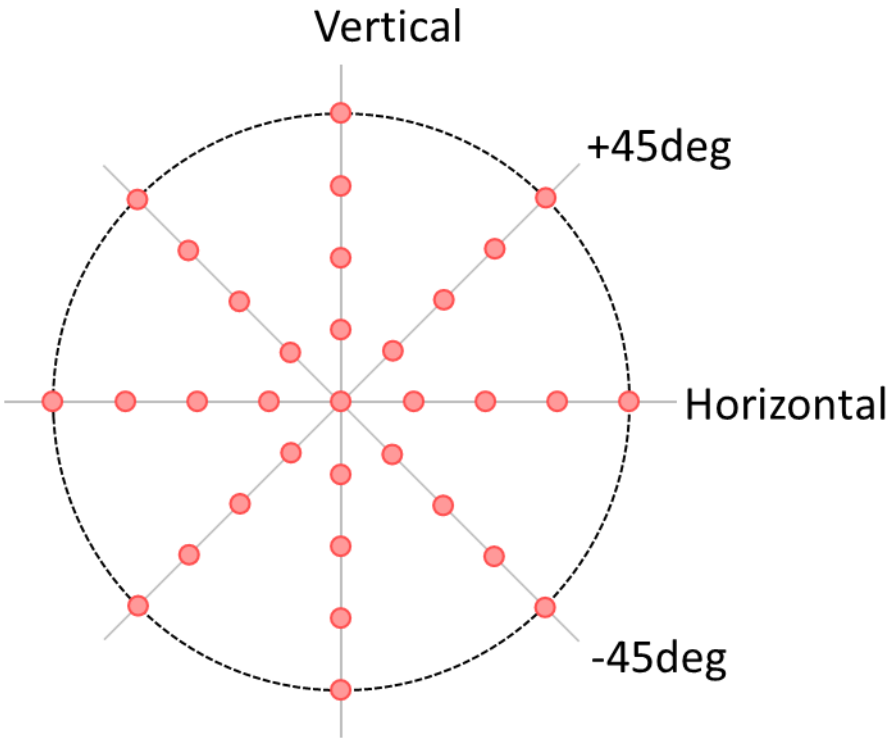

A summary of the configurations to be tested is shown in Table F.5-1 for z=0:

Table F.5-1: Tested Configurations

Test Data No.	Field Probe Scan Direction	Probe Polarization	Feed Polarization	Phase Scan
1	Horizontal	H	H	β (Scan=1)
2	Horizontal	V	V	β (Scan=2)
3	Vertical	H	H	β (Scan=3)
4	Vertical	V	V	β (Scan=4)
5	+45°	H	H	β (Scan=5)
6	+45°	V	V	β (Scan=6)
7	-45°	H	H	β (Scan=7)
8	-45°	V	V	β (Scan=8)

The basic measurement procedure is as follows:

1. Align the axes of the positioner to the range coordinate system.
2. Mount the reference AUT at the position (0, 0, 0) -> center of coordinate system.
3. Align the AUT V polarization to the feed V polarization.
4. Measure the phase at (0, 0, 0). If using a Network Analyzer for the field probing procedure, this measurement can be a 2-port calibration in order to make all subsequent measurement points relative to this point.
5. Scan the AUT horizontally, vertically, +45°, and -45° in the xy plane. Mount the horn such that it remains co-polarized with the feed through the duration of the scan.
6. Record S21V (co-polarized) for each position on the all four lines (step 4) in the xy plane.
7. Change feed polarization to H-polarization.
8. Repeat step 2 to 5.
    a. At step 5, S21H (co-polarized) is recorded for each position on all four lines in the xy plane.
9. Move the AUT to next z position -> z=+14.15 cm.
10. Measure the phase at (0, 0, 14.15 cm) as described in step 4.
11. Repeat steps 5 through 8.
12. Move the AUT to next z position -> z=-14.15 cm.
13. Measure the phase at (0, 0, -14.15 cm) as described in step 4.
14. Repeat steps 5 through 8.

Alternatively, the use of a dual-polarized reference AUT is not precluded and a slightly modified procedure could be used.

The phase variations shall be evaluated for the combined field probing scans independently for each constant z, i.e., the phase variation due to the propagation in the z-direction shall not be compensated. The maximum phase variation for each fixed z is determined by combining (concatenating) all 8 scans performed at given z, e.g., Scan = {1, …, 8} at z = 0, and evaluating the total peak-to-peak variation. The maximum phase variation within the spherical quiet zone, $\Delta\beta_{max}$, shall be calculated and reported

using:

$$\Delta\beta_{\max} = \max\left[\Delta\beta(\text{Scan} = \{1,...,8\}, z = 0), \Delta\beta(\text{Scan} = \{1,...,8\}, z = -14.15\text{cm}), \Delta\beta(\text{Scan} = \{1,...,8\}, z = 14.15\text{cm})\right]$$

(EQUATION F.5)

where $\Delta\beta$ is the maximum phase variation within the concatenated linear scans performed at position z, i.e.,

$$\Delta\beta(\text{Scan}, z) = \max\left[\beta(\text{Scan}, z)\right] - \min\left[\beta(\text{Scan}, z)\right]$$

(EQUATION F.6)

where β are related to the S-parameter measurements as follows: $\beta_i = \angle[S21_H]$ for for Scans 1, 3, 5, and 7, and $\beta_i = \angle[S21_V]$ for Scans 2, 4, 6, and 8.

Note that it is necessary to unwrap the phase if any β has rolled over a 360° boundary, e.g. -180° to +180°.

F.6 Maximum Phase Variation

The maximum phase variation $\Delta\beta_{max}$ for the permitted methodology of IFF, determined either with the rotary scan or the field probing approach, shall be 22.5°. This maximum limit could be revisited based on OEM feedback on sensitivity of UE beam management to phase variation.

Revision History

Date	Version	Description
March 2020	1.0	Initial release
April 2020	1.0.1	• Minor editorial text changes made • Minor formatting changes made • Corrected Clenshaw-Curtis Weight equations • Corrected Influence of noise equation • Corrected broken reference links • Corrected numbering of Figure 7.7-1 and Figure 7.7-2 and Figure 7.7-3 • Section 5: Corrected "Appendix D.2," "Appendix D.3," and "Appendix D.4" references